Supporting Information for:

Chemical Switching Behaviour of Tricarbonylrhenium(I) Complexes of a New Redox Active 'Pincer' Ligand.

Sarath Wanniarachchi,[a] Brendan J. Liddle[a] John Toussaint,[a] Sergey V. Lindeman,[a] Brian Bennett[b] and James R. Gardinier*[a]

Department of Chemistry, Marquette University, Milwaukee, WI 53201-1881.

[b]*Department of Biophysics, Medical College of Wisconsin, Milwaukee, WI, USA 53226.*

Table of Contents:

[1] *Experimental. General Considerations.* S-4

[3] *Spectroscopic and Electrochemical Characterization.*

Experimental Section

General Considerations. The compounds pyrazole, CuI, N,N'-dimethylethylenediamine (DMED), anhydrous K_2CO_3 powder, Tl(X = PF_6 or OTf) and $(NEt_4)(OH)$ (1M in MeOH) were purchased from commercial sources and used without further purification while $Re(CO)_5Br$,[S1] di(2-bromo-4-tolyl)amine,[S2] were prepared by literature methods. The solvents used in the preparations were dried by conventional methods and distilled prior to use. Midwest MicroLab, LLC, Indianapolis, Indiana 45250, performed all elemental analyses. IR spectra were recorded in the 4000-500 cm^{-1} region (as KBr pellets or as CH_2Cl_2 solutions in a cell with KBr windows) on a Nicolet Magna-IR 560 spectrometer. ^1H and ^{13}C NMR spectra were recorded on a Varian 400 MHz spectrometer. Chemical shifts were referenced to solvent resonances at δ_H 7.27, δ_C 77.23 for $CDCl_3$; δ_H 5.33, δ_C 54.00 for $CDCl_3$; δ_H 1.94, δ_C 118.9 for CD_3CN and δ_H 2.05, δ_C 29.92 for acetone-d_6. Melting point determinations were made on samples contained in glass capillaries using an Electrothermal 9100 apparatus and are uncorrected. Absorption measurements were recorded on an Agilent 8453 spectrometer. Electrochemical measurements were collected under nitrogen atmosphere at a scan rate of 100 mV/s for samples as 0.1 mM CH_2Cl_2 solutions with 0.1 M NBu_4PF_6 as the supporting electrolyte. A three-electrode cell comprised of an Ag/AgCl electrode (separated from the reaction medium with a semipermeable polymer membrane filter), a platinum working electrode, and a glassy carbon counter electrode was used for the voltammetric measurements. With this set up, the ferrocene/ferrocenium couple had an $E_{1/2}$ value of +0.53 V consistent with the literature value in this solvent.[S3] Mass spectrometric measurements recorded in ESI(+) or ESI(-) mode were obtained on a Micromass Q-TOF spectrometer whereas that performed by using direct-probe analyses were made on a VG 70S instrument. For the ESI(+) experiments, formic acid (approximately 0.1 % v/v) was added to the mobile phase (CH_3CN). EPR measurements were obtained using a Bruker ELEXSYS E600 equipped with an ER4116DM cavity resonating at 9.63 GHz, an Oxford Instruments ITC503 temperature controller and ESR-900 helium-flow cryostat. The ESR spectra were recorded with 100kHz field modulation.

Syntheses.

Di(2-(pyrazolyl)-4-tolyl)amine, H(L). A mixture of 10.82 g (0.030 mol) di(2-bromo-p-tolyl)amine, 7.25 g (0.107mol, 3.5 equiv) pyrazole, 14.72 g (0.107mmol, 3.5 equiv) K_2CO_3, 1.2 mL (0.012 mol, 40 mol %) DMED, and 10 mL of distilled xylenes was purged with nitrogen 15 min. Then, 0.58 g (3 mmol, 10 mol %) CuI was added as a solid under nitrogen and the mixture was heated at reflux for 36 h under nitrogen. After cooling to room temperature, 200 mL of H_2O was added and the mixture was extracted with three 100 mL portions of CH_2Cl_2. The combined organic layers were dried over $MgSO_4$, filtered, and solvent was removed by rotary evaporation to give an oily residue that was purified by column chromatography on silica gel. Elution using 10:1 hexanes:ethyl acetate (R_f = 0.5) afforded 6.90 g (69 %) of **H(L)** as a white powder, after removing solvent and drying under vacuum. Mp, 89 - 90 ^oC. Anal. Calcd (obs.) for $C_{20}H_{19}N_5$: C, 72.93 (73.05); H, 5.81 (5.97); N, 21.26 (20.88). ^1H NMR: (CD_2Cl_2) 8.48 (s, 1H, NH), 7.72 (dd, *J* = 2, 0.6 Hz, 2H, H_3pz), 7.67 (dd, *J* = 2, 0.6 Hz, 2H, H_5pz), 7.25 (d, *J* = 8 Hz, 2H, Ar), 7.12 (s, 2H, Ar), 7.03 (d, *J* = 8 Hz, 2H, Ar), 6.43(dd, *J* = 2, 0.6 Hz, 2H, H_4pz), 2.30 (s, 6H, $ArCH_3$). ^1H NMR (acetone-d_6) : 8.72 (s, 1H, NH), 7.94 (dd, *J* = 2, 0.6 Hz, 2H, H_3pz), 7.81 (dd, *J* = 2, 0.6 Hz, 2H, H_5pz), 7.36 (d, *J* = 8 Hz, 2H, Ar), 7.29 (d, *J* = 2 Hz, 2H, Ar), 7.19 (dd, *J* = 8, 2 Hz, 2H, Ar), 6.57 (dd, *J* = 2, 0.6 Hz, 2H, H_4pz), 2.41 (s, 6H, $ArCH_3$). ^{13}C NMR: ($CDCl_3$) 140.5, 134.7, 130.7, 130.2, 130.1, 129.0, 125.8, 118.9, 106.7, 20.6. UV-VIS λ_{max}, nm (ε, $M^{-1}cm^{-1}$), CH_2Cl_2: 238 (31,600), 303 (22,700). LRMS (Direct Probe) m/z (Int.) [assign.]: 329 (100) $[HL]^+$, 262 (8)

$[HL–Hpz]^+$, 173 (15) $[H_2L–pztolyl]^+$. Single crystals suitable for X-ray diffraction were obtained by slow cooling a hot hexanes solution (supersaturated) to room temperature over the course of a few hours.

***fac*-ReBr(CO)$_3$[H(L)]**, **1**. A mixture of 0.510 g (1.27 mmol) $Re(CO)_5Br$ and 0.455g (1.38 mmol) of **H(L)** in 20 mL toluene was heated at reflux 15 h. The resulting precipitate was isolated by filtration, washed with two 5 mL portions Et_2O and dried under vacuum which afforded 0.71 g (83 %) of **1** as a colorless solid. Mp. 272 - 274°C dec. Anal. Calcd (obs.) for $C_{23}H_{19}BrN_5O_3Re$: C, 40.65 (40.33); H, 2.82 (2.67); N, 10.31 (10.02). IR (KBr) ν_{co} 2020, 1920, 1880 cm^{-1}. IR (CH_2Cl_2) ν_{co} major bands; 2029, 1919, 1896, minor bands; 2038, 1930 cm^{-1}. ^1H NMR: (CD_2Cl_2, 293K): (three species, see text: **I**, 48% of signal integration intensity from well-resolved resonances in the $ArCH_3$, NH, and H_4pz regions of the spectrum; **II**, 42% of signal; **III** 10 % of signal): 11.92 (s, 1H, NH, **II**), 11.40 (s, 1H, NH, **III**), 9.89 (s, 1H, NH, **I**), 8.22 (d, *J* = 3 Hz, 1H, H_5pz, **III**), 8.18 (d, *J* = 3 Hz, 1H, H_5pz, **I**), 8.17 (d, *J* = 2 Hz, 1H, H_3pz, **I**), 8.13 (d, *J* = 2 Hz, 1H, H_3pz, **III**), 8.01 (d, *J* = 3 Hz, 1H, H_5pz, **III**), 7.92 (d, *J* = 2 Hz, 2H, H_3pz, **II**), 7.91(d, *J* = 3 Hz, 3H, H_5pz, **I** and **II**), 7.90 (d, *J* = 2 Hz, 1H, H_3pz, **III**), 7.88 (d, *J* = 3 Hz, 1H, H_5pz, **I**), 7.59-7.54 (m, Ar, 2H, **I**/**II**/**III**), 7.48 (s, 1H, Ar, **III**), 7.36-7.31 (m, Ar, 3H, **I**/**II**/**III** and H_5pz, **I**), 7.30 (s, 1H, Ar, **III**), 7.23-7.08 (m, 2.5H, Ar **I**/**II**/ **III**), 6.86 (d, *J* = 8 Hz, 1H, Ar, **III**), 6.77 (dd, *J* = 3, 2 Hz, 1H, H_4pz, **I**), 6.76 (dd, *J* = 3, 2 Hz, 1H, H_4pz, **III**), 6.61 (dd, *J* = 3, 2 Hz, 1H, H_4pz, **III**), 6.51 (dd, *J* = 3, 2 Hz, 2H, H_4pz, **II**), 6.41 (dd, *J* = 3, 2 Hz, 1H, H_4pz, **I**), 5.94 (d, *J* = 8 Hz, 1H, Ar, **III**), 2.51 (s, 3H, $ArCH_3$, **III**), 2.47 (s, 3H, $ArCH_3$, **I**), 2.44 (s, 3H, $ArCH_3$, **I**), 2.37 (s, 6H, $ArCH_3$, **II**), 2.32 (s, 3H, $ArCH_3$, **III**). ^{13}C NMR: (CD_2Cl_2, 293K) major asymmetric species **I**: 148.00, 141.34, 139.05, 137.68, 135.23, 133.52, 132.09, 128.34, 124.69, 122.81, 119.92, 110.5, 108.37, 21.31, 20.93; symmetric species **II**: 148.85, 139.13, 136.45, 132.97, 130.57, 124.78, 124.24, 110.06, 20.98; minor asymmetric species **III**: 148.89, 142.41, 140.10, 136.93, 136.76, 135.07, 134.99, 131.72, 131.27, 131.06, 130.27, 128.39, 124.74, 124.15, 122.87, 110.53, 108.40, 21.26, 20.91. UV-VIS λ_{max}, nm (ε, $M^{-1}cm^{-1}$), CD_2Cl_2: 230 (49,300), 251 (32,300), 287 (11,100). LRMS ESI(+) m/z (Int.) [assign.]: 743 (4) $[ReBr(CO)_3(HL)+Na(CH_3CN)]^+$, 721 (6) $[ReBr(CO)_3(H_2L)+ CH_3CN]^+$, 718 (7) $[ReBr(CO)_3(HL)+K]^+$, 702 (5) $[ReBr(CO)_3(HL)+Na]^+$, 641 (1) $[Re(CO)_3(H_2L)+CH_3CN]^+$, 600 (100) $[Re(CO)_3(HL)]^+$, 330 (31) $[H_2L]^+$. X-ray quality crystals were grown by layering an acetone solution with hexane and allowing the solvents to slowly diffuse over two days.

$\{Re(CO)_3[H(L)]\}(PF_6)$, 2·PF_6. A mixture of 0.208 g (0.306 mmol) of **1** and 0.107 g (0.306 mmol) $TlPF_6$ in 20 mL dry CH_3CN was heated at reflux for 15 h. After cooling to room temperature, TlBr was removed by filtration through Celite, and solvent was removed from the filtrate by rotary evaporation. The residue was washed with two 5 mL portions of Et_2O and was dried under vacuum to give 0.184 g (80 %) of **2·PF_6** as a white powder. Mp, 255 – 258 °C dec. Anal. Calcd (obs.) for $C_{23}H_{19}F_6N_5O_3PRe$: C, 37.10 (36.99); H, 2.57 (2.32); N, 9.41 (9.16). IR (KBr) ν_{co} 2040, 1950, 1930 cm^{-1}. ^1H NMR: (CD_2Cl_2, 293K) 7.95 (d, *J* = 2 Hz, 2H, H_3pz), 7.91 (d, *J* = 3 Hz, 2H, H_5pz), 7.74 (s, 1H, NH), 7.24-7.16 (m, 4H, Ar), 6.58 (dd, *J* = 3, 2 Hz, 2H, H_4pz), 2.41 (s, 6H, $ArCH_3$). ^{13}C NMR: suitable spectrum of a concentrated solution could not be obtained even after 24 hours acquisition time. UV-VIS λ_{max}, nm (ε, $M^{-1}cm^{-1}$), CD_2Cl_2: 230 (42,500), 245 (34,800), 367 (1,750). LRMS ESI(+) m/z (Int.) [assign.]: 600 (100) $[(HL)Re(CO)_3]^+$. X-ray quality crystals were grown by layering a dichloromethane solution with hexane and allowing the solvents to slowly diffuse over two days.

$\{Re(CO)_3[H(L)]\}(OTf)$, 2·OTf. A mixture of 0.175 g (0.258 mmol) of **1** and 0.091 g (0.26 mmol) TlOTf in 20 mL dry CH_3CN was heated at reflux for 15 h. After cooling to room temperature, TlBr was removed by filtration through Celite, and solvent was removed from the filtrate by rotary evaporation. The residue was washed with two 5 mL portions of Et_2O and was dried under vacuum to give 0.173 g (90 % based on **1**) of **2·OTf** as a white powder. Mp, 275 - 277°C dec. Anal. Calcd (obs.) for $C_{24}H_{19}F_3N_5O_6ReS$: C, 38.50 (38.78); H, 2.56 (2.72); N, 9.35 (8.99). IR (CH_2Cl_2) ν_{co} 2040, 1938, 1922 cm^{-1}. IR (KBr) ν_{co} 2036, 1947, 1922 cm^{-1}. ^1H NMR: (CD_2Cl_2, 293K) 9.79 (s, 1H, NH), 7.93 (d, *J* = 2 Hz, 2H, H_3pz), 7.89 (d, *J* = 3 Hz, 2H, H_5pz), 7.25-7.15 (m, 6H, Ar), 6.55 (dd, *J* = 3, 2 Hz, 2H, H_4pz), 2.39 (s, 6H, $ArCH_3$). ^{13}C NMR: (CD_2Cl_2, 293K) 193.5, 191.3, 148.1, 139.5, 135.9, 133.2, 132.2, 130.7, 125.0, 123.9, 110.1, 21.0. UV-VIS λ_{max}, nm (ε, $M^{-1}cm^{-1}$), CD_2Cl_2: 230 (43,000), 245 (34,000), 367 (1,700). LRMS ESI(+) m/z (Int.) [assign.]: 600 (100) $[(HL)Re(CO)_3]^+$. X-ray quality crystals were grown by layering a dichloromethane solution with hexane and allowing the solvents to slowly diffuse over two days.

$Re(CO)_3(L)$, 3. To a solution of 0.105 g (0.15mmol) **1** in 20 mL of CH_3CN was added 1.50 mL of a 0.103 M $(NEt_4)(OH)$ solution in MeOH (0.155 mmol), immediately giving a yellow solution. The mixture was stirred for 15 min then solvent was removed by rotary evaporation. The residue was washed with two 5 mL portions Et_2O, and the yellow product was extracted with three 10 mL portions of benzene. Benzene was removed by vacuum distillation to afford 0.060 g (67 %) of **3** as a yellow powder. Mp. 295-298°C dec. Anal. Calcd (obs.) for $C_{23}H_{18}N_5O_3Re$: C, 46.15 (45.89); H, 3.03 (3.11); N, 11.70 (11.58). IR (CH_2Cl_2) ν_{co} 2015, 1905, 1885 cm^{-1}. IR (KBr) ν_{co} 2013, 1901, 1876 cm^{-1}. ^1H NMR: (CD_2Cl_2, 293 K) 7.95 (d, *J* = 2 Hz, 2H, H_3pz), 7.92 (d, *J* = 3 Hz, 2H, H_5pz), 7.82 (part of AA'BB', 2H, Ar), 7.12 (part of AA'BB', 2H, Ar), 7.11 (s, 2H, Ar), 6.52 (dd, *J* = 3, 2 Hz, 2H, H_4pz), 2.36 (s, 6H, $ArCH_3$). ^1H NMR: (acetone-d_6) 8.35 (dd, *J* = 2, 1 Hz, 2H, H_3pz), 8.30 (dd, *J* = 2, 1 Hz, 2H, H_5pz), 7.84 (part of AB d, *J* = 8 Hz, 2H), 7.29 (d, *J* = 2, Hz, 2H, Ar), 7.11 (part of AB d, *J* = 9, 2 Hz, 2H, Ar), 6.65 (dd, *J*

= 2, 1 Hz, 2H, H_4pz), 2.31 (s, 6H, $ArCH_3$). ^{13}C NMR: (CD_2Cl_2) 196.8, 146.6, 142.9, 130.9, 130.3, 129.0, 128.0, 123.9, 119.4, 108.0, 20.7. HRMS [Direct Probe, m/z] Calc. (Obs) for $C_{23}H_{18}N_5O_3Re$: 599.0968 (599.0973). LRMS (Direct Probe) m/z (Int.) [assign.]: 599 (30) $[LRe(CO)_3]^+$, 515 (58) $[LRe – 3 CO + H]^+$, 329 (28) $[H_2L]^+$, 173 (100) $[H_2L–pztolyl]^+$, 105 (47) $[H_2Ntolyl]^+$. UV-VIS λ_{max}, nm (ε, $M^{-1}cm^{-1}$), CD_2Cl_2: 229 (40,200), 239 (37,900), 309 (10,600), 353 (8,500), 390 (6,400) . X-ray quality crystals were grown by layering an acetone solution with hexane and allowing the solvents to slowly diffuse over two days.

Acid/base cycling experiments.

UV-Vis spectroscopic experiments. In a typical UV-Vis spectroscopic acid/base cycling experiment, 10 μL aliquots of 1.904 m$\underline{M}$ acid (HBF_4 or CF_3COOH) in CH_2Cl_2 solution were sequentially added to 3.0 mL of a 0.0635 m$\underline{M}$ $ReLCO_3$ solution in CH_2Cl_2 where the disappearance of the band at 450 nm was monitored. After one equivalent of acid was added, 10 μL aliquots of 1.904 m$\underline{M}$ $(NEt_4)(OH)$ solution in dichloromethane were added to the resultant solution. This acid/base cycle was repeated three more times.

Electrochemical experiments. In a representative acid/base cycling experiment monitored by cyclic voltammetry, a solution of 0.0100 g (0.0167 mmol) of $Re(CO)_3$(**L**) (**3**) and 0.300 g (1.23 mmol) NBu_4PF_6 in 15 mL dry CH_2Cl_2 was treated with 10 μL aliquots of 0.1670 $\underline{M}$ tetrafluoroboric acid in CH_2Cl_2 where the cyclic voltommogram was recorded between 0.0 to +1.0 V versus Ag/AgCl (the potential values in the main text were calibrated to an external Fc/Fc^+ couple +0.53 V versus Ag/AgCl in CH_2Cl_2) at a scan rate of 100 mV/s after each addition. After the wave centered near +0.53 V versus Ag/AgCl, indicative of **3**, approached a constant near zero baseline current value (after approximately one equivalent of acid added), 10 μL aliquots of 0.1670 M $(NEt_4)(OH)$ in CH_2Cl_2 were added. The voltammograms recorded after each successive base addition, as above. This acid/base cycling process was repeated three more times.

Chemical Oxidation of 3.

Spectrophotometric Titrations. Standard solutions the cation radical 9,10-dimethoxyocta-hydro-1,4:5,8-dimethanoanthracenium hexachloroantimonate, (**CRET**$^+$)(**SbCl**$_6^-$),[S4] were prepared by dissolving the cation radical in freshly distilled CH_2Cl_2 and diluting until the absorbance measured at 517 nm was about 1.0, corresponding to a concentration of $1.37x10^{-4}$ M (ε 7,300). For the titrations, 3 mL of this standard solution were used and the spectrum was acquired before and after the addition 10 μL aliquots of 0.00548 M solutions of **3**.

Synthetic Scale. A solution of 0.054g (89 μmol) of (**CRET**$^+$)(**SbCl**$_6^-$) in 15 mL dry, distilled CH_2Cl_2 and the resultant solution was transferred under nitrogen by cannula to a magnetically stirred solution of 0.053 g (89 μmol) **3** in 15 mL CH_2Cl_2. The resultant royal blue solution was stirred 10 min and solvent was removed under vacuum. The blue solid was washed with two 5 mL portions of pentane and then dried under vacuum to give 0.053 g (64 %) of (**3**$^+$)(**SbCl**$_6^-$) as a blue solid.

Alternatively, a solution of 0.115 g (0.448 mmol) AgOTf in 10 mL CH_2Cl_2 was added to a solution of 0.268 g (0.447 mmol) **3** in 10 mL CH_2Cl_2. After the resulting blue-black mixture had been stirred 1 h, the blue solution was separated from silver metal by filtration. Solvent was removed by vacuum distillation and the blue residue was washed with two 5 mL portions of hexane to leave 0.244 g (73% based on Re) of (**3**$^+$)(**OTf**$^-$) as a blue solid. IR (CH_2Cl_2) ν_{co} 2035, 1932, 1925 cm^{-1}. IR (KBr) ν_{co} 2031, 1941 cm^{-1}. UV-VIS λ_{max}, nm (ε, M^{-1}cm^{-1}), CD_2Cl_2: 488 (1,000), 618 (2,680), 748 (3,600), 892sh (900), 1046sh (460).

Crystallography.

X-ray intensity data from a colorless block of **H(L)**, a colorless plate of ReBr(CO)$_3$[**H**(**L**)] (**1**), a colorless prism of {Re(CO)$_3$[**H(L)**]}(PF$_6$), (**2·PF$_6$**), a colorless prism of {Re(CO)$_3$[**H(L)**]}(OTf), (**2·OTf**), and a yellow block of Re(CO)$_3$(**L**), (**3**) were measured at 100(2) K with a Bruker AXS 3-circle diffractometer equipped with a SMART2[S5] CCD detector using Cu(Kα) radiation. Raw data frame integration and Lp corrections were performed with SAINT+.[S6] Final unit cell parameters were determined by least-squares refinement of 7538, 6621, 8198, 9905, and 7176 reflections from the data sets of **H(L), 1**, **2·PF$_6$**, **2·OTf**, and **3**, respectively, with $I > 2\sigma(I)$ for each. Analysis of the data showed negligible crystal decay during collection in each case. Direct methods structure solutions, difference Fourier calculations and full-matrix least-squares refinements against F^2 were performed with SHELXTL.[S7] Semi-empirical absorption correction based on the multiple measurement of equivalent reflections was applied to the data of **H(L)** with SADABS.[S6] An empirical absorption correction of area-detector data for twinned (2:1 component ratio separated by ca 2 degree split) crystals and of **1** was applied with TWINABS.[S6] Numerical absorption corrections based on the real shape of the crystals for the remainder of the compounds were applied with SADABS.[S6] All non-hydrogen atoms were refined with anisotropic displacement parameters with the following exception. Two alternative positions of PF_6^- anion were found in **2·PF$_6$** from a series of difference Fourier syntheses and were refined with soft geometric restraints (using the SAME instruction in SHELXL). Their relative population was refined to 27/73. The fluorines of the minor disorder component were refined isotropically. The secondary amino nitrogens in **H(L)** and in **2·X** (X =

PF_6, OTf) were located and refined whereas the remaining hydrogen atoms in all complexes were placed in geometrically idealized positions and included as riding atoms. The X-ray crystallographic parameters and further details of data collection and structure refinements are presented in Table S-1. Selected bond distances and interatomic angles are found in Table S-2 while the remaining distances and angles can be found in the cif files deposited with the CSD.[S8]

Table S-1. Crystallographic Data and Refinement Parameters for **H(L)**, ReBr(CO)$_3$[**H**(**L**)] (**1**), {Re(CO)$_3$[**H(L)**]}(X) (X = PF$_6$, **2·PF$_6$**; X = OTf, **2·OTf**), and Re(CO)$_3$(**L**), (**3**).

Compound	**H(L)**	**1**	**2·PF$_6$**	**2·OTf**	**3**
Formula	$C_{20}H_{19}N_5$	$C_{23}H_{19}BrN_5O_3Re$	$C_{23}H_{19}F_6N_5O_3PRe$	$C_{24}H_{19}F_3N_5O_6ReS$	$C_{23}H_{18}N_5O_3Re$
Formula weight	329.40	679.54	744.60	748.70	598.62
Crystal system	Monoclinic	Monoclinic	Monoclinic	Monoclinic	Monoclinic
Space Group	P n	P 2$_1$/c	P 2$_1$/c	P 2$_1$/n	C 2/c
a, Å	7.3364(2)	8.1846(4)	15.6722(7)	8.1784(2)	24.5632(5)
b, Å	16.5933(4)	31.9302(14)	9.6375(4)	18.4766(4)	11.8412(3)
c, Å	14.1016(3)	8.9168(5)	16.8562(7)	17.1772(4)	15.4073(3)
α, deg	90	90	90	90	90
β, deg	98.6740(10)	102.901(3)	103.315(2)	90.9260(10)	110.1570(10)
γ, deg	90	90	90	90	90
V, Å^3	1697.03(7)	2271.5(2)	2477.53(18)	2595.29(10)	4206.86(16)
Z	4	4	4	4	8
T, K	100(2)	100(2)	100(2)	100(2)	100(2)
ρ calcd, Mg m^{-3}	1.289	1.987	1.996	1.916	1.890
λ(Cu Kα), Å	1.54178	1.54178	1.54178	1.54178	1.54178
μ, mm^{-1}	0.631	12.830	10.967	10.561	11.611
Abs. Correction	multi-scan	multi-scan	numerical	numerical	numerical
F(000)	696	1304	1440	1456	2320
θ range [°]	2.66 to 66.41	2.77 to 67.93	2.90 to 67.71	3.51to 67.78	3.83 to 67.85
Reflns collected	13695	35582	20721	21636	17421
Indep. reflns	2889 (R_{int} 0.0242)	4046(R_{int} 0.1068)	4328(R_{int} 0.0372)	4638(R_{int} 0.0197)	3759(R_{int} 0.0199)
T_min/max	0.7865/0.9513	0.2060/0.6279	0.3627/0.6744	0.1306/0.4336	0.1143/0.2748
Data/restraints/ parameters	2889/2/464	4046/0/300	4328/21/392	4638/0/367	3759/0/292
Goodness-of-fit on F^2	0.985	1.042	1.009	1.022	1.002
R[I>2σ(I)][c](all data)	0.0282 (0.0292)	0.0438 (0.0467)	0.0267 (0.0321)	0.0196 (0.0205)	0.0172 (0.0173)
*w*R[d] (all data)	0.0731 (0.0738)	0.1059 (0.1073)	0.0657 (0.0678)	0.0509 (0.0514)	0.0489 (0.0490)

$R = \Sigma||F_o|-||F_c||/\Sigma|F_o|$. [d]$wR = [\Sigma w(|F_o^2|-|F_c^2|)^2/\Sigma w|F_o^2|^2]^{1/2}$

Figure S-1. Structure Diagrams with Atom Labeling of ReBr(CO)$_3$[**H**(**L**)] (**1**), {Re(CO)$_3$[**H(L)**]}(PF$_6$) (**2·PF$_6$**) {Re(CO)$_3$[**H(L)**]}(OTf) (**2·OTf**), and Re(CO)$_3$(**L**), (**3**).

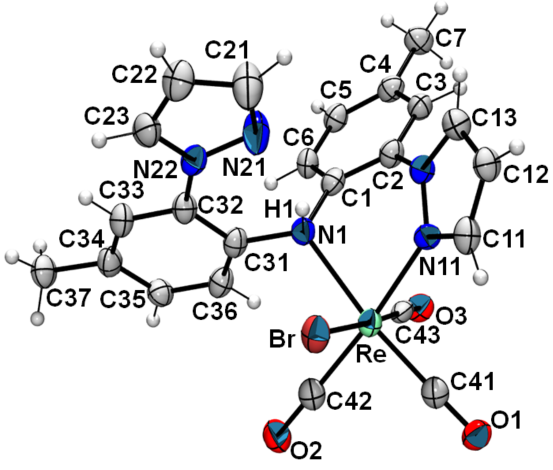

(**1**)

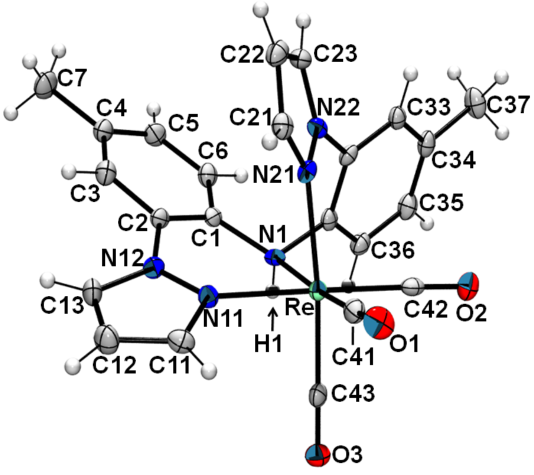

(**2·PF$_6$**)

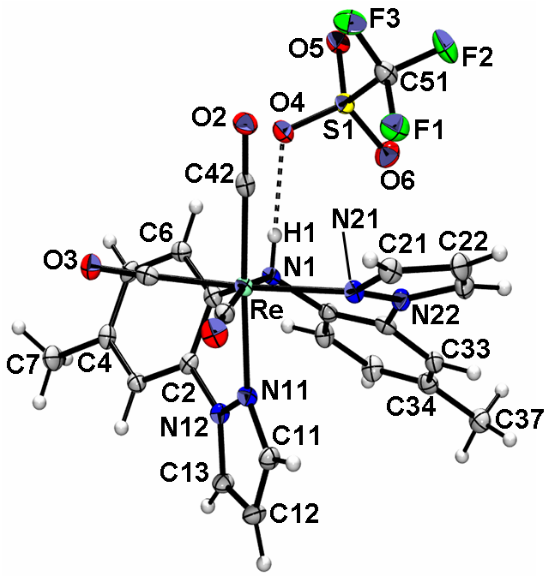

(**2·OTf**)

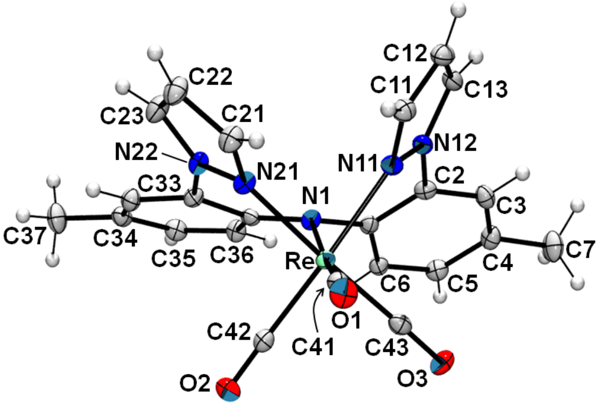

(**3**)

Table S-2. Summary of Bond Distances and Angles in Rhenium Complexes **1**-**3**.

Distance (Å)	**1**	**2·PF$_6$**	**2·OTf**	**3**
Re-Br	2.619	---	---	---
Re-N1	2.265	2.257	2.249	2.163
Re-N11	2.182	2.174	2.169	2.173
Re-N21	---	2.180	2.174	2.148
Re-C41	1.899	1.915	1.910	1.914
Re-C42	1.928	1.944	1.936	1.923
Re-C43	1.946	1.933	1.933	1.948
C41-O1	1.164	1.149	1.150	1.158
C42-O2	1.142	1.129	1.144	1.147
C43-O3	1.091	1.140	1.139	1.138
N1H1•••N21(or O4)	1.913		2.014	
⊥N1•••(C_2Re)[a]	0.383	0.492	0.488	0.191
Angles/torsions (°)				
N1-Re-N11	77.15	77.75	76.61	79.26
N1-Re-N21	---	83.68	83.76	81.57
Fold (N11)[b]	138.81	130.62	123.45	136.17
Fold (N21)[c]	---	159.24	154.62	147.36
ReN11-N12C2	-16.09	14.07	0.61	-14.34
ReN21-N22C32	---	-9.76	-18.36	8.35
pz(N11)-tol(C1)	40.80	43.63	32.29	45.04
pz(N21)-tol(C31)	13.63	27.21	29.82	36.32
tol(C1)- tol(C31)	76.86	74.55	76.03	28.43
Σ∠'s about N1[d]	344.44	334.46	334.85	355.62

pz = mean plane of pyrazolyl ring , tol = mean plane of C_6 ring of tolyl group; [a] Distance of normal vector between N1 and mean plane of atoms Re, C1, and C31; [b] fold angle between Re and the centroids (Ct) of N1 and N11 and Ct of C1 and N12; [c] fold angle between Re and the centroids (Ct) of N1 and N21 and Ct of C31 and N22; [d] involving Re, C1, and C31.

Spectroscopic and Electrochemical Characterization.

Figure S-3. Overlay of IR spectroscopic data for carbonyl stretching region of **1** obtained from (a) KBr pellets and (b) from CH_2Cl_2 solutions.

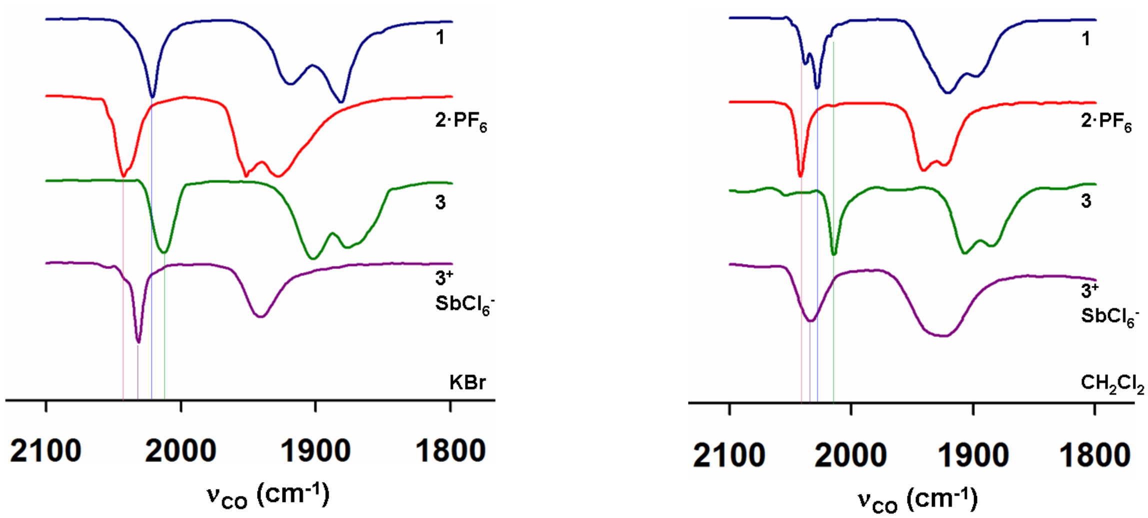

(a) (b)

Figure S-4. Top: Cyclic voltammograms of **3** in CH_2Cl_2 with NBu_4PF_6 as supporting electrolyte recorded at 100 mV/s. Bottom: Scan rate dependence of **3** in CH_2Cl_2 and in CH_3CN

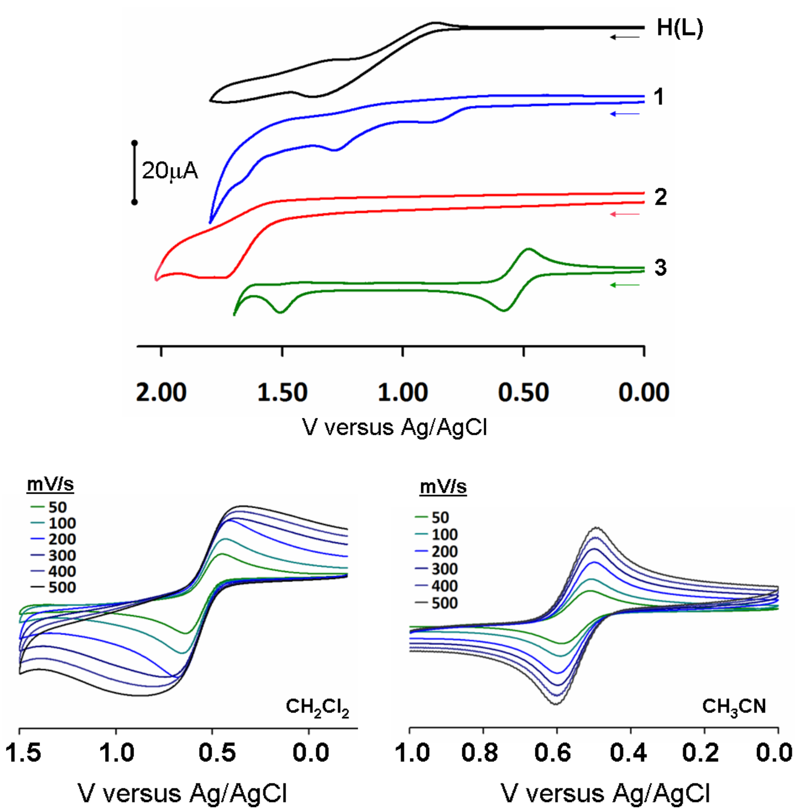

Figure S-5. Overlay of the electronic absorption spectra of each **1** and **2·PF$_6$** in CD$_2$Cl$_2$ at 293 K

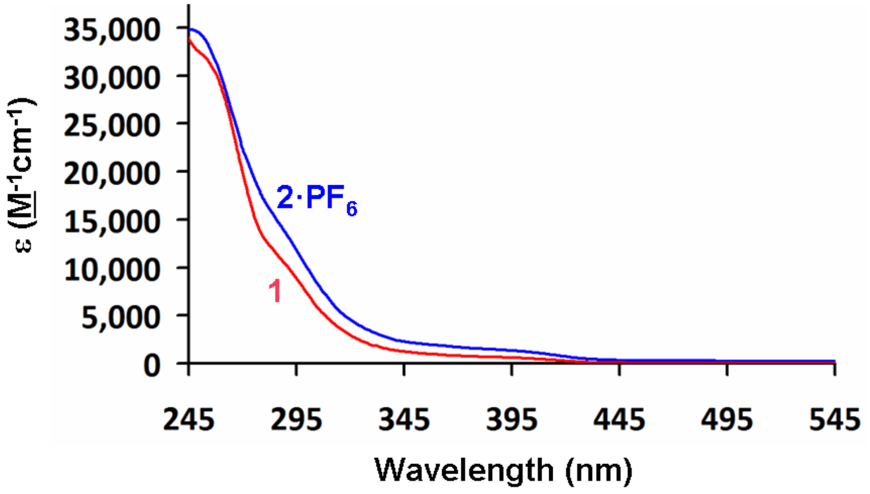

Figure S-6. ESI(+) mass spectrum of **1** (CH$_3$CN).

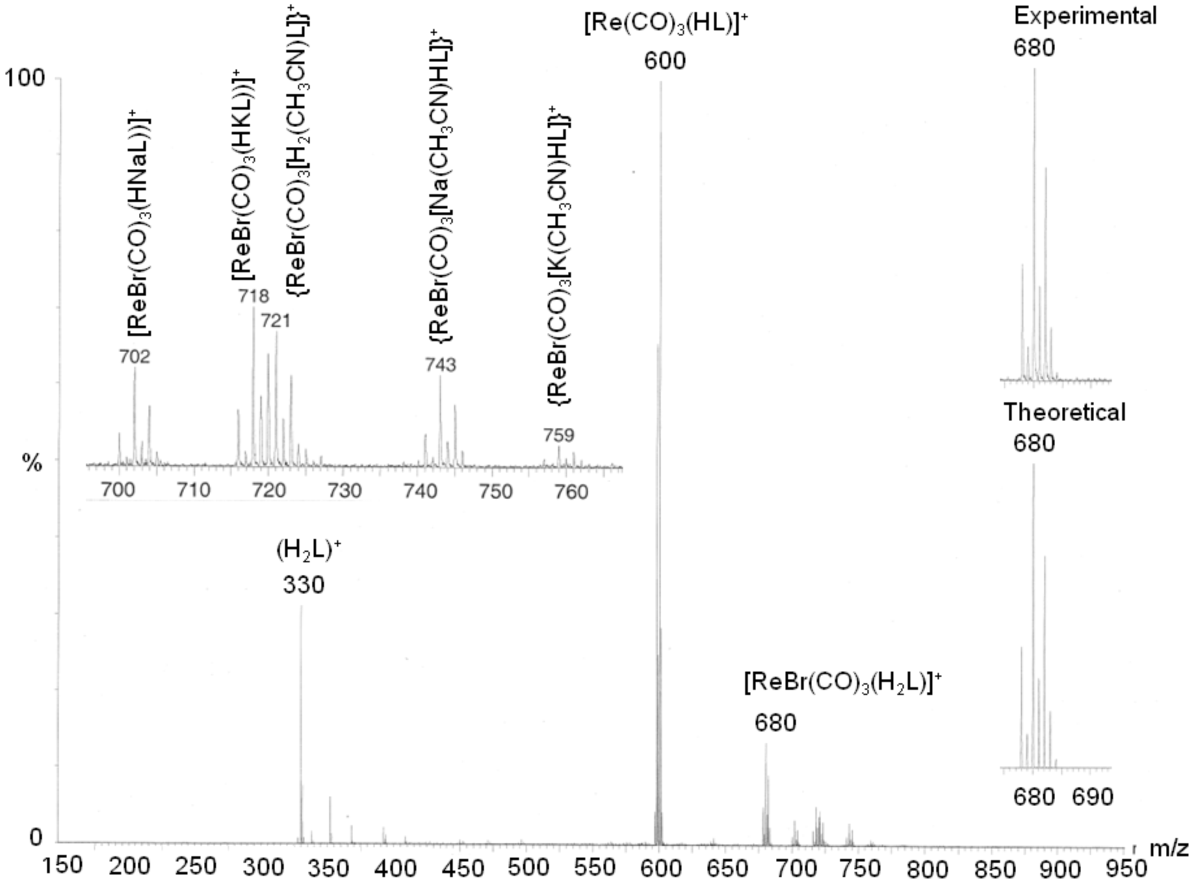

Figure S-7. ESI(+) mass spectrum of **2·PF$_6$** (CH$_3$CN).

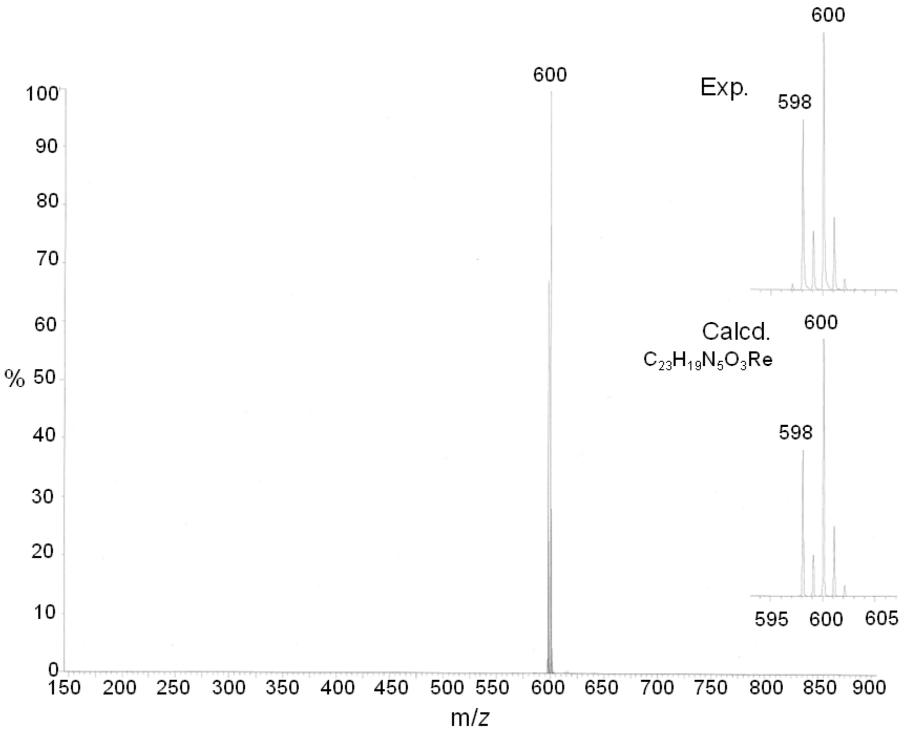

Figure S-8. Direct Exposure Probe (EI) mass spectrum of **3**.

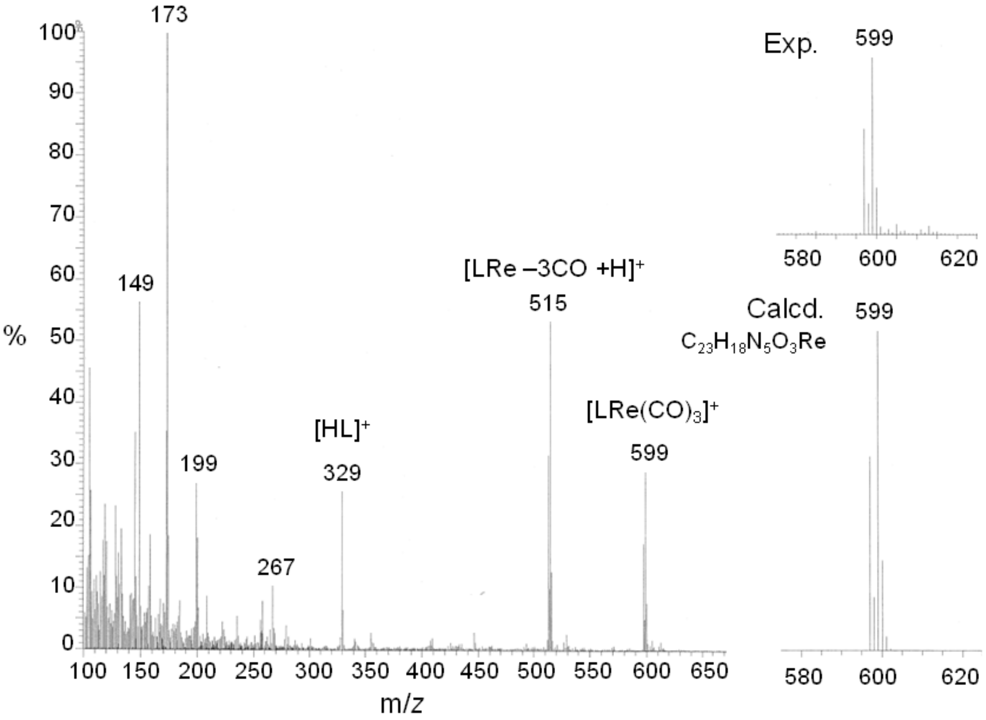

Figure S-9. The 400 MHz ^{1}H NMR spectrum of **1** in CD_2Cl_2 (*) at 293 K with three main species **I** (major asymmetric), **II** (Symmetric), **III** (minor asymmetric) easily identified in the N-H, H_4pz, and CH_3 regions.

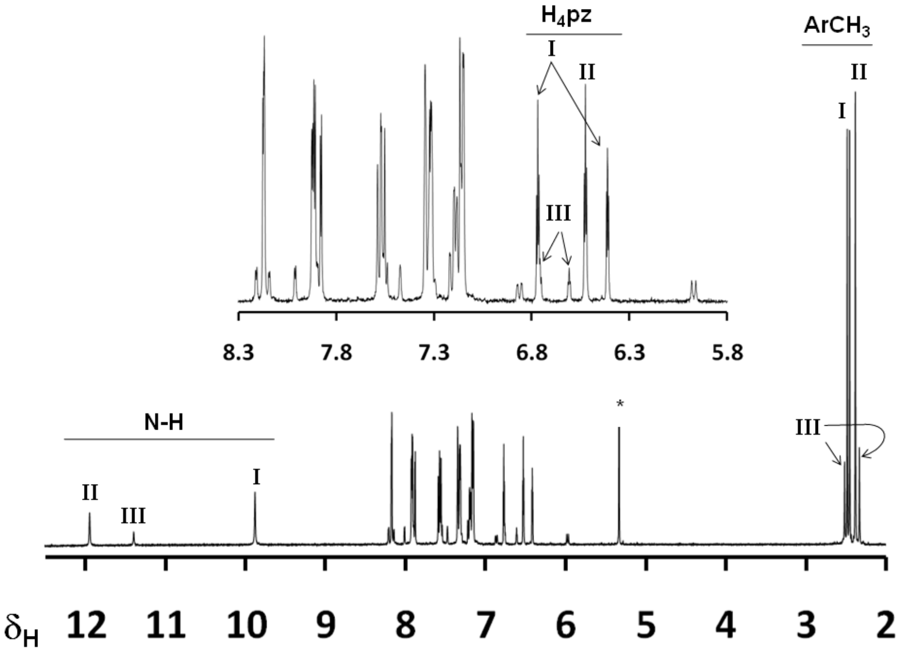

Figure S-10. The aromatic region of the DQCOSY ^{1}H NMR spectrum (400 MHz) of **1** in CD_2Cl_2 at 293 K.

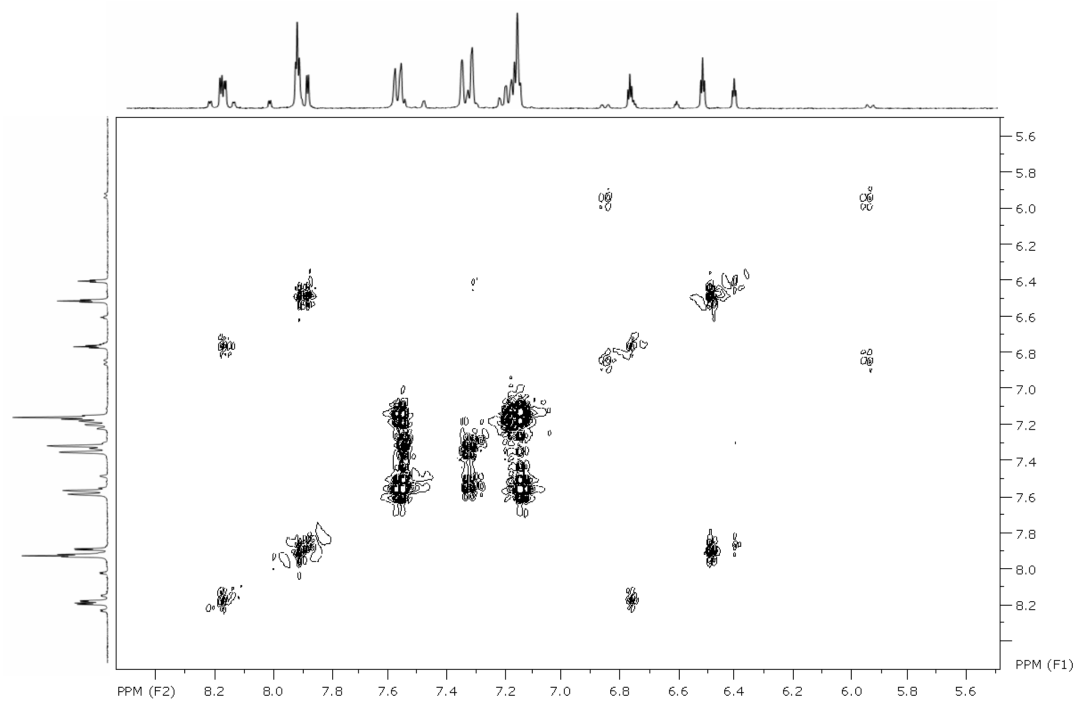

Figure S-11. General features of variable temperature ^{1}H NMR spectra of **1** in (a) CD_2Cl_2 (δ_H = 5.33 ppm) and in (b) $C_2D_2Cl_4$ (aromatic region emphasized, with NH region inset). Red squares: Major asymmetric species, **I**; Blue circles: symmetric species, **II**; green triangles: Minor asymmetric species, **III**.

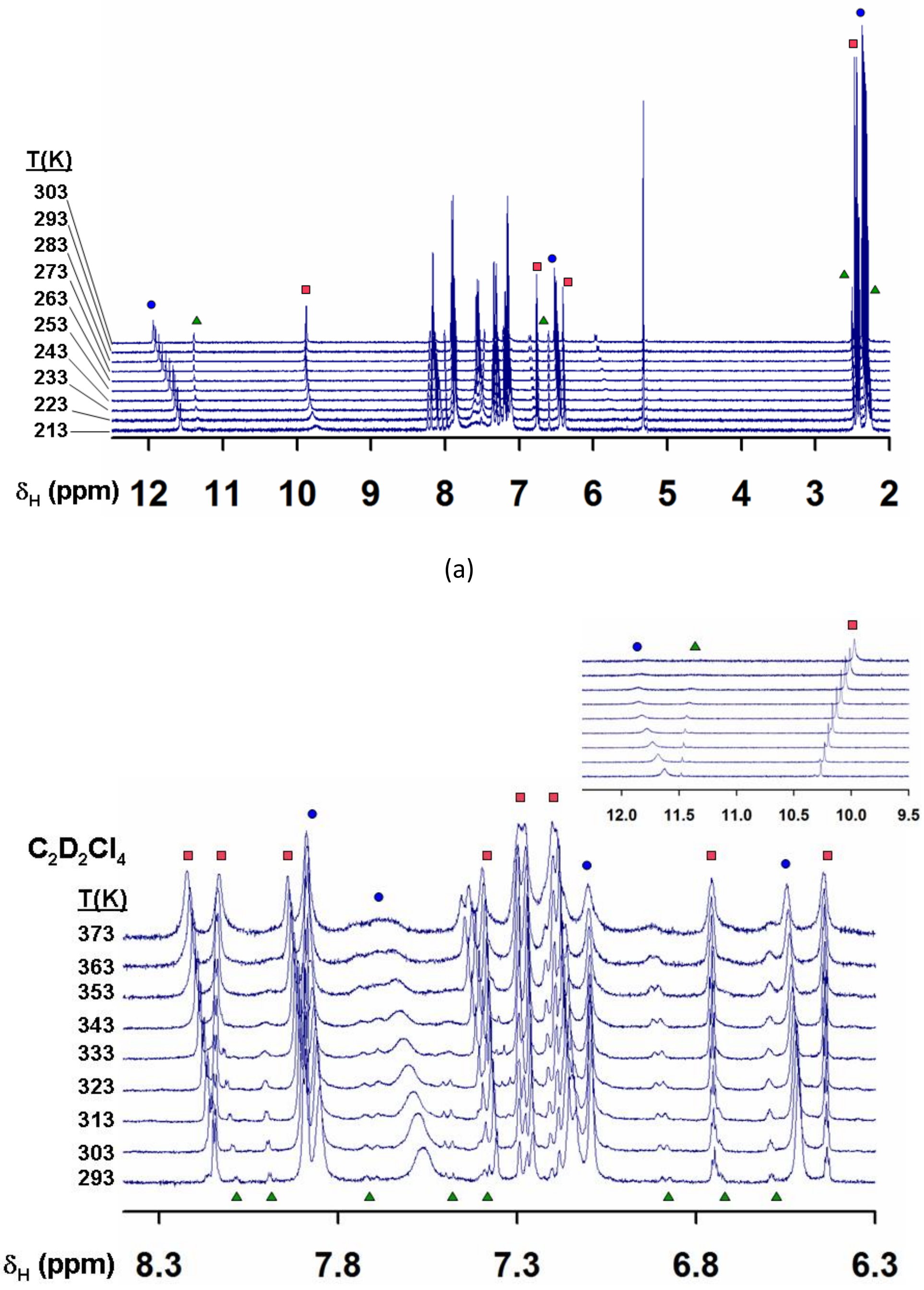

(b)

Figure S-12. Relative composition of three species as a function of temperature, obtained by averaging the relative integrations of N-H, H_4pz, and CH_3- regions of the ^{1}H NMR spectra, of **1** in (a) CD_2Cl_2 and (b) $C_2D_2Cl_4$.

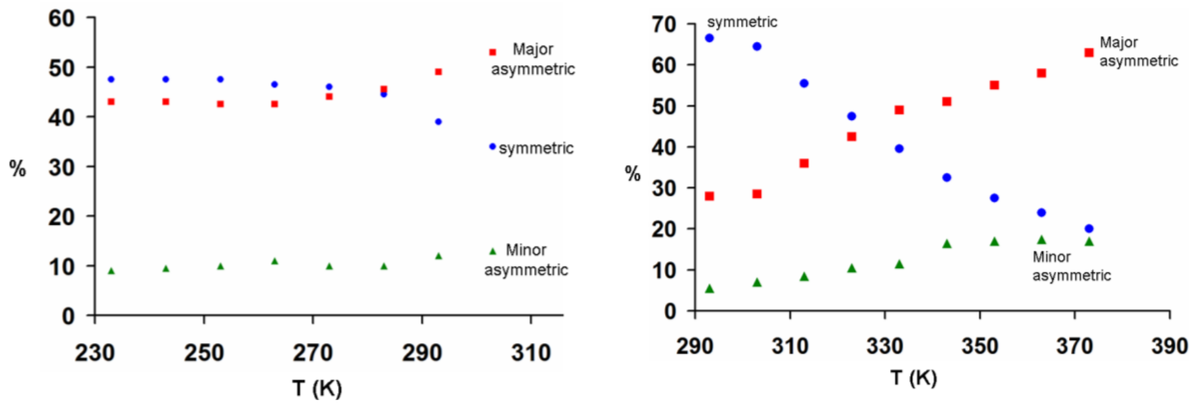

(a) (b)

Figure S-13. Variable temperature ^{1}H NMR spectra of (a) **2·PF$_6$** and (b) **2·OTf** in CD_2Cl_2.

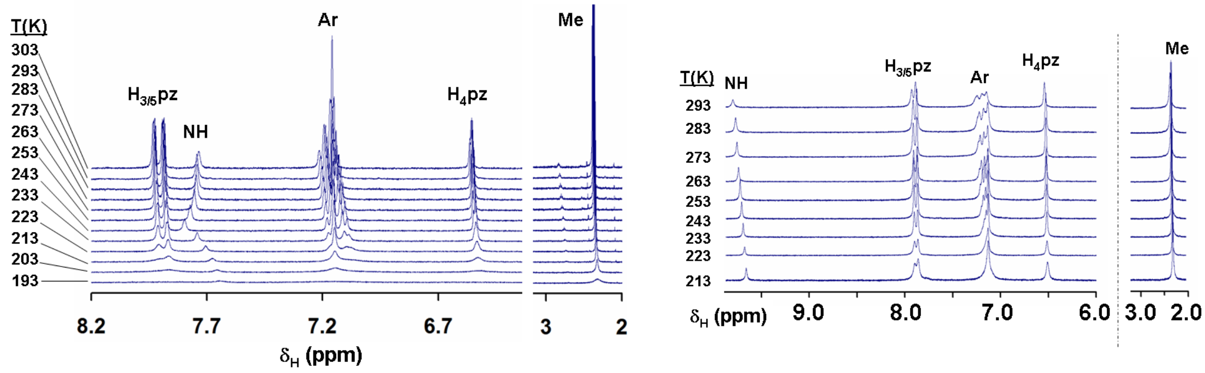

(a) (b)

Figure S-14. Variable temperature ^{1}H NMR spectrum of **3** in CD_2Cl_2.

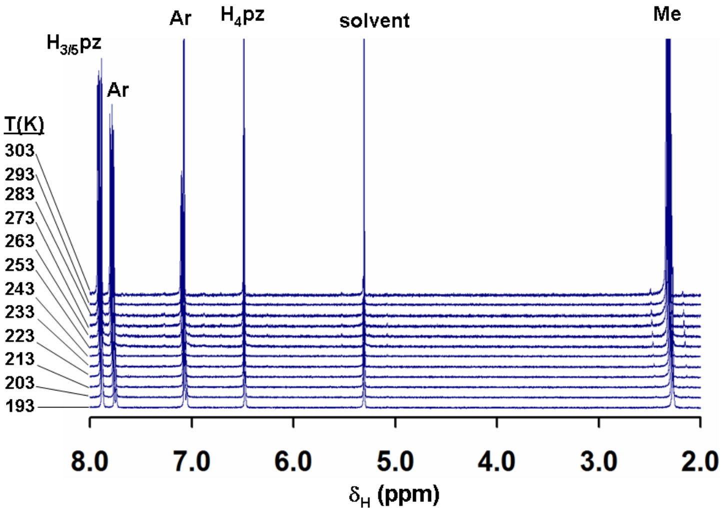

Table S-3. Summary of room temperature (293 K) ^{1}H NMR chemical shift data (CD_2Cl_2).

	H(L)	$Re(CO)_3Br[H(L)]$ (**1**)			$[Re(CO)_3[H(L)]]^+$ (**2**)		$Re(CO)_3L$ (**3**)
Assign		symm	asym min	asym maj	OTf^-	PF_6^-	
NH	8.48	11.92	11.40	9.89	9.79	7.77	---
H_3pz bnd		7.92	8.13	8.17	7.93	7.95	7.95
H_3pz unb	7.72		7.90	7.31			
H_5pz bnd		7.91	8.22	8.18	7.89	7.92	7.92
H_5pz unb	7.68		8.01	7.88			
H_4pz bnd		6.51	6.76	6.77	6.55	6.58	6.51
H_4pz unb	6.43		6.61	6.41			
Ar_{AB} bnd		7.57	6.86	7.58	7.26	7.22	7.81
Ar_{AB} unb	7.25		7.55	7.21			
$Ar_{AB'}$ bnd		7.32	5.94	7.18	7.19	7.18	7.12
$Ar_{AB'}$ unb	7.03		7.35	7.14			
Ar-H bnd		7.36	7.48	7.35	7.15	7.17	7.10
Ar-H unb	7.12		7.09	7.17			
CH_3 bnd		2.37	2.51	2.47	2.39	2.41	2.36
CH_3 unb	2.30		2.32	2.44			

Discussion of NMR spectra and solution structures of 1-3.

The ^{1}H NMR spectrum of pure **1** in various solvents is much more complicated than anticipated from the solid state structure owing to the presence of three species tentatively assigned based on comparison of solution properties [NMR, IR, CV, UV, ESI(+)] of related species and on molecular modeling, as arising from different (interconvertible) geometric and coordination isomers of ReBr(CO)$_3$[**H(L)**], shown in Scheme S-1. That is, if the solid state structure of **1** were retained in solution (similar to the right of Scheme S-1), the ^{1}H NMR spectrum would be expected to give a single resonance for the N-H group and two sets of signals for each pyrazolyl and tolyl groups arising from the asymmetric nature of ligand bonding (one rhenium-bound and one unbound arm of the ligand). Instead, three species are found in the NMR spectrum of **1** in CH$_2$Cl$_2$ (and other chlorinated solvents) that are most easily distinguished by the three resonances above 9 ppm for a nitrogen-bound hydrogen of each (lower left of Figure S-9 with assignments in Table S-3). By relative integration, these three species occur in a 48:42:10 ratio at room temperature. Accordingly, there are resonances for three different species in the higher field regions of the NMR spectrum. The second most intense set of resonances corresponds to a symmetric species, presumably [*fac*-Re(CO)$_3$[H(L)]$^+$}(Br$^-$) (left of Scheme S-1, vide infra), that shows only a single set of resonances each for pyrazolyl and tolyl group hydrogens. Although the structure on the left of Scheme S-1, appears asymmetric, it is noted that the ^{1}H NMR spectra of **2·X** (X = PF$_6$, OTf) that have similar solid state structures each show a symmetric ligand environment due to rapid conformational processes that did not reach the slow exchange limit even at -80°C (Figure S-13). Moreover, the chemical shifts of the symmetric bromide species are quite similar to the latter two complexes (Table S-3) where subtle differences are anticipated by the presence of different anions. There are two other species that occur in an approximate 4:1 ratio whose signals are consistent with an asymmetric ligand binding environment (with two sets of pyrazolyl and two sets of tolyl hydrogen resonances for each species). The number or resonances and their chemical shifts are consistent with the expectations described above for **1**, if the solution structures of each species were similar to the

Scheme S-1. Different low-energy (MMFF) geometric and coordination isomers of ReBr(CO)$_3$[**H(L)**].

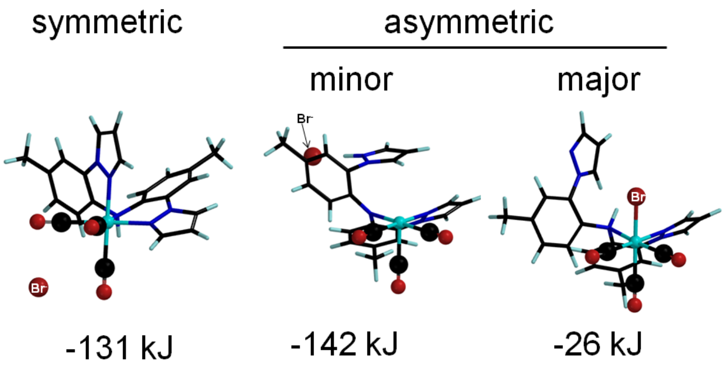

solid state. The resonances in the region 6.0 to 6.7 ppm for 4-pyrazolyl hydrogens and in the region 2.2 to 2.5 ppm for tolyl-CH_3 hydrogens are sufficiently resolved (Figure S-9) to allow relative integrations which reproduce the 48 (symmetric): 42 (major asymmetric): 10 (minor asymmetric) ratio observed in the N-H region of the spectrum and also allow assignments to the latter hydrogens. The resonances for the remaining hydrogens of each species could be assigned by examining the cross-peaks in the DQCOSY ^1H NMR spectrum (Figure S-10), by their temperature dependence, as well as by comparison of chemical shifts and relative intensities in different solvents Figures S-11 to S-14), features that will be elaborated on in the full paper. The signals for the major asymmetric species are most likely due to the intact complex **1** (right of Figure) on the basis of IR, cyclic voltammetry and to a lesser extent ESI(+) mass spectrometry for CH_3CN solutions. That is the solid state IR spectrum (Figure S-3, left) for **1** consists of an intense sharp single A_1 (if one assumes C_{3v} local symmetry) C-O stretch at 2020 cm^{-1} which is in between that for **2·X** (2042 cm^{-1}) and **3** (2013 cm^{-1}), as expected. On the other hand, the solution (CH_2Cl_2) spectrum of **1** (Figure S-3, right) consists of three sharp A_1 (if one assumes C_{3v} local symmetry) C-O stretches at 2038, 2029, and 2017 cm^{-1} (minor). The first band is consistent with the energy range for **2·X** and the lowest-energy minor band consistent with the deprotonated amido **3;** the intense band at 2029 is likely due to intact **1**. Moreover, the cyclic voltammogram of **1** recorded in CH_2Cl_2 (Figure S-4) shows an irreversible wave with E_{pa} near +0.86 V (vs Ag/AgCl) due to the Br^-/Br^o couple, a fairly high-current irreversible wave with E_{pa} near +1.26 V consistent with other (NN-L)Re^IBr/(NN-L)$Re^{II}Br$ couples, and a more intense irreversible wave with E_{pa} near +1.26 V consistent with cationic (NN-L)Re^I/(NN-L)Re^{II} couples.[S9] The ESI spectrum of **1** (Figure S-6) also shows that the parent ion (100% relative intensity) at m/z = 600 is due to $\{[H(L)]Re(CO)_3]\}^+$ but even under these conditions peaks for intact **1** and those for intact **1** bound to various cations present (H^+, Na^+, K^+) under the conditions of the experiment (arising from the spectrometer, not impurities in the sample) are still observed. The assignment of the third (minor asymmetric) species as being due to the species in the middle of Scheme S-1 is the most tentative of the assignments, which is based on the observations from simple molecular mechanics modeling (MMFF) which identified this species as the lowest-energy structure of the multitude examined. This species can be considered as an intermediate arising from the ionization of **1** to give species such as **2**. An alternative assignment of the minor asymmetric species being due to different conformers of intact **1** where the axial and bromide groups are exchanged such that N-H and Re-CO are in the same direction with HN-ReC torsion near 0^o or a conformer with a *fac*-$Re(CO)_3$ kernel possessing a HN-ReBr torsion of 90^o was disfavored as these conformers were found to be nearly isoergonic, separated only by about 2 kcal in energy (with the latter being lowest energy), but cannot be excluded. Moreover, *trans*-$Re(CO)_3$ isomers seemed also less likely considering that only *fac*- isomers were ever observed throughout the series of coordination complexes of this ligand. This latter assignment and the mechanistic features for the interconversions of species will be probed in greater detail in the full paper that describes the effects of 3-pyrazolyl substitution on the properties of the complexes.

Figure S-15. Spectrophotometric titration of **3** in CH_2Cl_2 using $(CRET^+)(SbCl_6^-)$ showing uncluttered character of one-electron transfer.

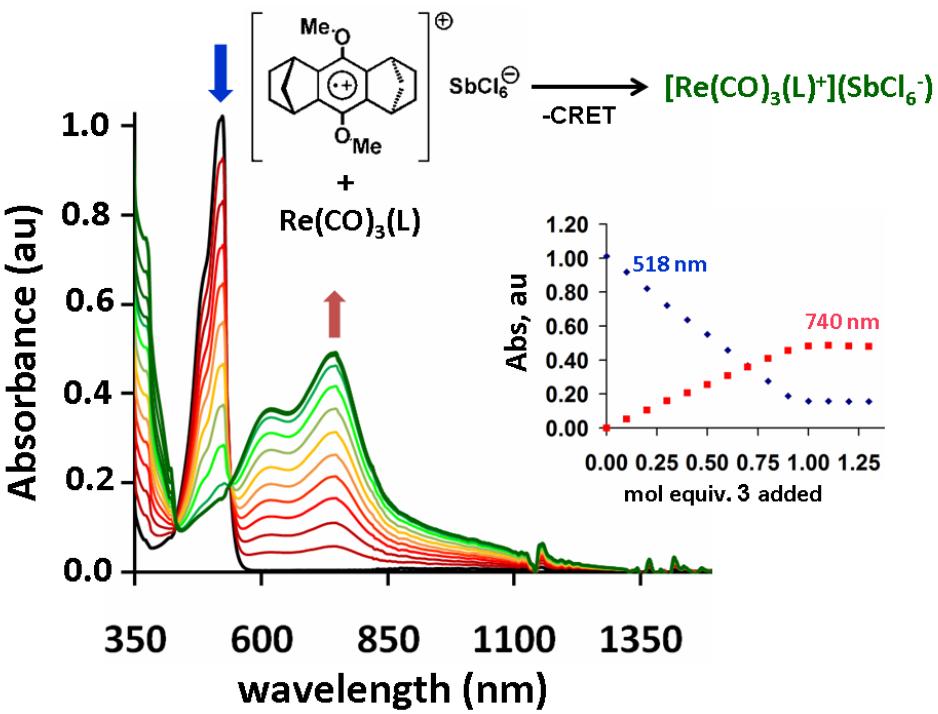

Computational Details. Calculations utilized the SPARTAN'08 program suite,[S10] where gas phase structures of the metal complexes were optimized using the BP86/6-31G* density functional theoretical model owing to the demonstrated success of this model when applied to other complexes.[S11] In the current cases, the structures all possess C_1symmetry and the agreement between this model and solid state structures was very good with the computational model closely replicating the main features of the solid state structures but with bond distances generally between 0.01 Å to 0.05 Å longer than experimental structures. Single point energy and time-dependent density functional calculations were performed on the energy-minimized structures using the hybrid B3LYP method, which incorporates Becke's three-parameter exchange functional (B3)[S12] with the Lee, Yang, and Parr (LYP)[S13] correlation functional where the LACVP* effective core potential[S14] basis set was employed. The time-dependent density functional calculations were performed on the six lowest-energy singlet and six-lowest energy triplet excited states of each complex **1**, $\mathbf{2}^+$, and **3**, but only the first six excited doublet states of $\mathbf{3}^+$ and the results are summarized in Figures S-17 to S-22 as well as in Tables S-9, pp S-39 to S-42.

Figure S-16. Overlay of experimental (green) and calculated structures ((u)BP86/LACVP*) for **3** (black) and **3^+** (pink) (hydrogens removed for clarity) and selected interatomic distances and angles tabulated.

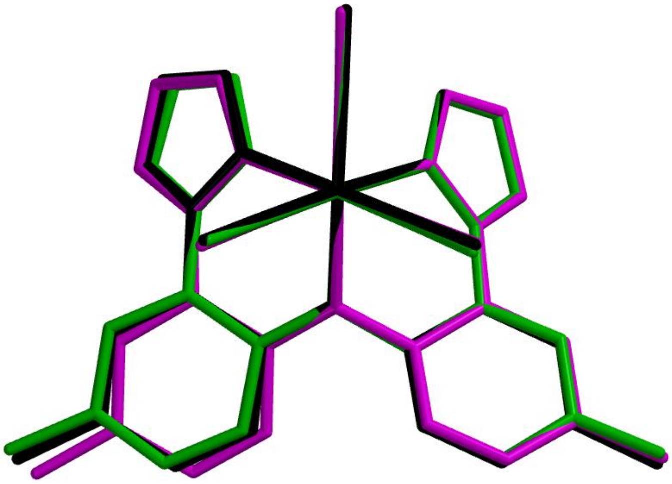

	Experimental	Calculated [(U)BP86/LACVP*]	
	3	**3**	**3^+**
Re-N_{Ar} (Å)	2.163	2.185	2.148
Re-N_{pz} (Å)	2.161	2.199	2.193
Re-C_{avg} (Å)	1.928	1.926	1.940
ReN-NC (^{o})	11.3	10.5	8.7
pz-tolyl (^{o})	36.3	38.7	36.7
tolyl-tolyl (^{o})	28.4	37.5	42.6

Table S-4. Cartesian coordinates for calculated structure of **1**.

```
Coordinates (Angstroms)
I Atom      X           Y           Z
-------------------------------------
1 Re   0.804133   -1.224656   -0.676135
2 Br  -0.694322   -2.280073    1.257486
3 O   -1.161920   -2.330919   -2.797152
4 O    2.472404    0.204259   -2.854470
5 O    2.506622   -3.779384   -0.951285
6 N    2.006854   -0.455066    1.000443
7 N    2.201575    0.877639    1.287682
8 N  -1.511707     1.352923    2.387420
9 N   -2.638084    0.853845    1.779690
10 N  -0.329236    0.729218   -0.046409
11 H  -0.398499    0.573295    0.984891
12 C   2.589132   -1.137528    2.004698
13 H   2.528249   -2.224300    2.009906
14 C   3.174575   -0.257860    2.939513
15 H   3.702386   -0.517524    3.854875
16 C   2.905278    1.015385    2.458082
17 H   3.119570    2.004269    2.857802
18 C   1.786274    1.929999    0.419018
19 C   2.649982    3.026311    0.253090
20 H   3.636590    2.991598    0.727418
21 C   2.287308    4.137089   -0.525400
22 C   1.023940    4.109134   -1.143561
23 H   0.699404    4.959422   -1.754628
24 C   0.163676    3.013181   -1.000412
25 H  -0.815371    3.032810   -1.484549
26 C   0.525179    1.900997   -0.225098
27 C   3.236715    5.299003   -0.721307
28 H   2.702706    6.265056   -0.684879
29 H   3.738398    5.242197   -1.705782
30 H   4.024457    5.315726    0.050624
31 C  -1.698128    1.109914    3.694981
32 H  -0.926422    1.410413    4.404620
33 C  -2.934036    0.466368    3.945232
34 H  -3.343107    0.139521    4.899682
35 C  -3.508882    0.309435    2.692489
36 H  -4.431011   -0.175762    2.379947
37 C  -2.798975    0.916708    0.367024
38 C  -4.107225    1.006450   -0.149105
39 H  -4.942797    1.083675    0.554608
40 C  -4.363734    1.027360   -1.527848
41 C  -3.261298    0.965674   -2.403764
42 H  -3.422923    0.968742   -3.487394
43 C  -1.958051    0.880373   -1.906915
44 H  -1.111281    0.804190   -2.596203
45 C  -1.700567    0.857510   -0.525206
46 C  -5.777502    1.141148   -2.055155
47 H  -6.518360    0.816380   -1.304952
48 H  -5.916632    0.524498   -2.960228
49 H  -6.021084    2.185123   -2.331174
50 C  -0.415472   -1.907277   -1.996151
51 C   1.840833   -0.335511   -2.015656
52 C   1.848365   -2.808719   -0.871043
```

Table S-5. Cartesian coordinates for calculated structure of **2**.

Coordinates (Angstroms)

I	Atom	X	Y	Z
1	Re	0.896247	-1.405138	-1.790988
2	O	3.942659	-0.837151	-1.665003
3	O	1.515581	-4.429957	-1.504601
4	O	1.091645	-1.556714	-4.867611
5	N	-1.255876	-1.905205	-1.860177
6	N	-2.140739	-1.841653	-0.804274
7	N	0.340544	0.712152	-1.728209
8	N	0.783622	1.556308	-0.733048
9	N	0.501160	-1.046798	0.466095
10	H	0.677169	-1.961632	0.909176
11	C	-1.818881	-2.746152	-2.756312
12	H	-1.288006	-2.979530	-3.677804
13	C	-3.054467	-3.233771	-2.293301
14	H	-3.720043	-3.937512	-2.788840
15	C	-3.228330	-2.645530	-1.050207
16	H	-4.020090	-2.750727	-0.312053
17	C	-2.038550	-0.915712	0.279478
18	C	-3.252771	-0.371433	0.752268
19	H	-4.171483	-0.587754	0.198598
20	C	-3.319272	0.455167	1.883978
21	C	-2.109661	0.755000	2.539551
22	H	-2.112779	1.388042	3.433581
23	C	-0.895199	0.262565	2.055585
24	H	0.032849	0.521023	2.573610
25	C	-0.828085	-0.564253	0.919628
26	C	-4.640203	0.992795	2.384026
27	H	-5.435188	0.896711	1.626474
28	H	-4.559878	2.056544	2.666698
29	H	-4.968754	0.441801	3.284963
30	C	-0.453404	1.460998	-2.520483
31	H	-0.927616	1.002963	-3.387388
32	C	-0.527276	2.787395	-2.049510
33	H	-1.090173	3.614302	-2.477527
34	C	0.268011	2.813409	-0.910880
35	H	0.492742	3.609602	-0.203632
36	C	1.716283	1.124789	0.257149
37	C	2.778692	1.968375	0.614826
38	H	2.883205	2.932281	0.104757
39	C	3.735301	1.576352	1.572206
40	C	3.599584	0.301825	2.156493
41	H	4.333589	-0.036786	2.895457
42	C	2.540747	-0.548801	1.807789
43	H	2.451956	-1.534223	2.281011
44	C	1.591857	-0.150134	0.858663
45	C	4.903021	2.474371	1.911601
46	H	5.250824	2.309045	2.944826
47	H	4.644762	3.540660	1.799721
48	H	5.758470	2.270099	1.240570
49	C	2.790134	-1.039285	-1.705012
50	C	1.287013	-3.288326	-1.635174
51	C	1.049054	-1.510397	-3.696744

Table S-6. Cartesian coordinates for calculated structure of **3**.

```
Coordinates (Angstroms)
I ATOM      X           Y           Z
-------------------------------------
1 Re  -0.192911    1.828400   -1.226229
2 O   -0.389511    4.857415   -1.872684
3 O    1.598964    1.320824   -3.702910
4 O   -2.699187    1.289640   -2.978442
5 N    1.549526    1.206831    0.438803
7 N   -1.383074    2.008199    0.636258
8 N   -2.072180    0.937867    1.158362
9 N   -0.015316   -0.180634   -0.384358
10 C   1.944861    3.324529    0.643890
11 H   1.398007    4.246036    0.451560
12 C   3.069798    3.091977    1.454291
13 H   3.605157    3.807327    2.075424
14 C   3.337686    1.735005    1.312385
15 H   4.075850    1.092968    1.785645
16 C   2.401846   -0.152017   -0.012498
17 C   3.652180   -0.802813   -0.056047
18 H   4.561126   -0.193458    0.007849
19 C   3.763231   -2.193346   -0.168494
20 C   2.553513   -2.921474   -0.183838
21 H   2.583988   -4.018395   -0.194590
22 C   1.313277   -2.287010   -0.216011
23 H   0.411651   -2.902703   -0.221048
24 C   1.174335   -0.864849   -0.234418
25 C  -1.472728    2.989482    1.556341
26 H  -0.992586    3.947947    1.367072
27 C  -2.217243    2.565835    2.675978
28 H  -2.447743    3.131424    3.576534
29 C  -2.580385    1.254972    2.389053
30 H  -3.134709    0.514017    2.961373
31 C  -2.311142   -0.255289    0.409445
32 C  -3.602587   -0.809648    0.442735
33 H  -4.386392   -0.294929    1.010573
34 C  -3.907321   -1.981075   -0.267201
35 C  -2.885083   -2.539851   -1.063433
36 H  -3.106220   -3.418883   -1.681619
37 C  -1.605997   -1.979004   -1.118632
38 H  -0.864670   -2.396831   -1.805172
39 C  -1.258538   -0.834867   -0.354410
40 C  -5.285192   -2.603764   -0.205612
41 H  -5.286968   -3.516625    0.420689
42 H  -5.639791   -2.899682   -1.209177
43 H  -6.026754   -1.907954    0.222762
44 C  -0.329125    3.696800   -1.665604
45 C   0.923408    1.519720   -2.762151
46 C  -1.757546    1.481688   -2.302013
47 C   5.108082   -2.879744   -0.264571
48 H   5.343511   -3.175922   -1.305346
49 H   5.925785   -2.222457    0.080079
50 H   5.134972   -3.800679    0.346083
-------------------------------------
```

Table S-7. Cartesian coordinates for calculated structure of **3**$^+$.

```
Coordinates (Angstroms)
I Atom      X           Y           Z
------------------------------------
1 Re   0.074210    1.139831    0.653655
2 O   -1.650633    0.695408    3.198864
3 O    0.151434    4.213500    1.145173
4 O    2.679575    0.831781    2.318335
5 N    1.206884    1.244810   -1.238673
6 N    1.918436    0.156220   -1.701383
7 N   -1.729535    1.320725   -0.549223
8 N   -2.588673    0.284651   -0.831331
9 N   -0.021263   -0.917670    0.047356
10 C   1.245239    2.156389   -2.231361
11 C   1.973462    1.671361   -3.336546
12 H   2.165561    2.177666   -4.280270
13 C   2.387601    0.399272   -2.965705
14 H   2.957982   -0.358461   -3.499689
15 C   2.245628   -0.948421   -0.857225
16 C   3.547770   -1.469251   -0.904026
17 H   4.282396   -1.005308   -1.570969
18 C   3.939601   -2.537334   -0.075155
19 C   2.986562   -3.051923    0.828655
20 H   3.276250   -3.849216    1.522059
21 C   1.683317   -2.547863    0.878662
22 H   0.979046   -2.925501    1.625957
23 C   1.272188   -1.509013    0.013768
24 C   5.357052   -3.059028   -0.100803
25 H   5.393282   -4.135175    0.137719
26 H   5.979038   -2.536434    0.650484
27 H   5.831588   -2.905163   -1.084233
28 C  -2.240653    2.407431   -1.160981
29 C  -3.421850    2.086328   -1.860090
30 H  -4.043012    2.749554   -2.458532
31 C  -3.612974    0.733611   -1.639176
32 H  -4.362548    0.046769   -2.023160
33 C  -2.440490   -1.051457   -0.363894
34 C  -3.612804   -1.819104   -0.274692
35 H  -4.581630   -1.313916   -0.330826
36 C  -3.585440   -3.216999   -0.121400
37 C  -2.315837   -3.849613   -0.124298
38 H  -2.255773   -4.942776   -0.085034
39 C  -1.146017   -3.107058   -0.144418
40 H  -0.185347   -3.624243   -0.125411
41 C  -1.151191   -1.672740   -0.148329
42 C  -4.853866   -4.017915    0.012605
43 H  -4.916342   -4.796923   -0.769619
44 H  -5.753269   -3.385376   -0.057522
45 H  -4.883768   -4.543413    0.985520
46 C  -0.999529    0.879440    2.245639
47 C   1.702874    0.942889    1.685353
48 C   0.138374    3.052514    0.994647
49 H  -1.737682    3.366889   -1.052348
50 H   0.750442    3.117956   -2.101853
------------------------------------
```

Table S-8. Calculated SCF and Frontier Orbital Energies (eV) for **1**, **2**, **3**, and $\mathbf{3}^{+}$.

	1	**2**	**3**	α-$\mathbf{3}^{+}$	β-$\mathbf{3}^{+}$
LUMO(+5)	+3.20	+0.63	+3.48	+0.33	+0.19
LUMO(+4)	+3.06	+0.42	+3.24	+0.11	+0.02
LUMO(+3)	+2.79	+0.21	+3.18	-0.24	-0.31
LUMO(+2)	+2.56	-0.10	+2.87	-0.42	-0.73
LUMO(+1)	+2.37	-0.50	+2.51	-0.84	-0.83
LUMO	+1.85	-0.74	+2.40	-1.17	-4.05
HOMO	-8.36	-10.99	-6.56	-11.40	-11.49
HOMO(-1)	-8.44	-11.16	-8.24	-11.71	-11.66
HOMO(-2)	-8.72	-11.49	-8.45	-11.93	-11.86
HOMO(-3)	-9.11	-11.67	-8.70	-12.39	-12.33
HOMO(-4)	-9.19	-11.93	-8.95	-12.41	-12.44
HOMO(-5)	-9.55	-12.13	-9.08	-12.66	-12.66
SCF energy(au)	-1470.20948	-1457.04671	-1456.63159	-1456.46797	

Fig. S-17. Frontier Orbitals for ReBr(CO)$_3$[(**HL**)] (**1**) from DFT calculations (B3LYP/LACVP*).

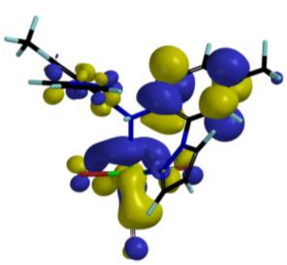	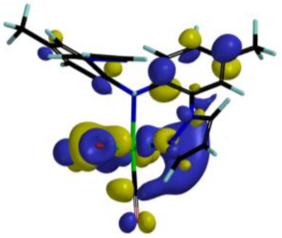	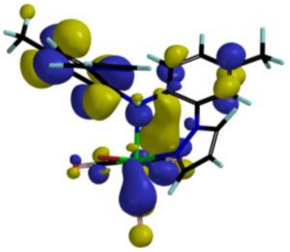
LUMO (+3)	**LUMO (+4)**	**LUMO (+5)**

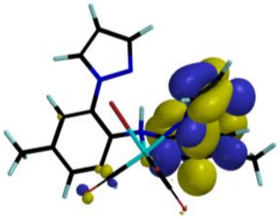	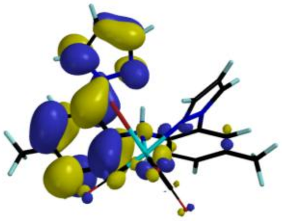	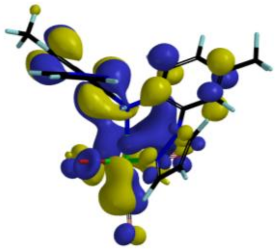
LUMO	**LUMO(+1)**	**LUMO(+2)**

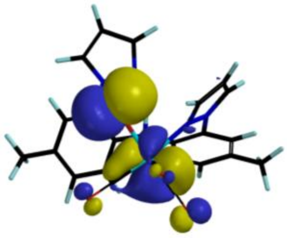	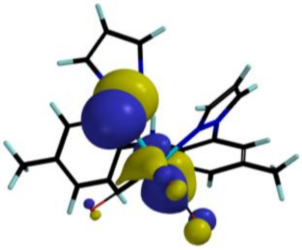	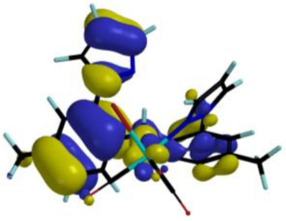
HOMO	**HOMO(-1)**	**HOMO(-2)**

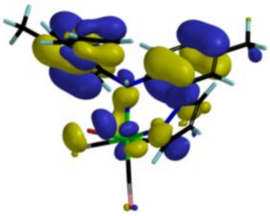	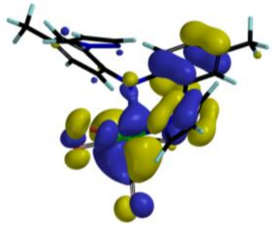	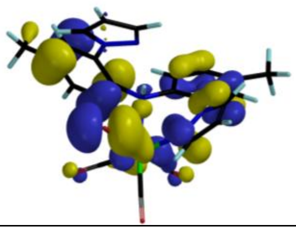
HOMO(-3)	**HOMO(-4)**	**HOMO(-5)**

Fig. S-18. Frontier Orbitals for $\{Re(CO)_3[(\mathbf{HL})]\}^+$ (**2**) from DFT calculations (B3LYP/LACVP*).

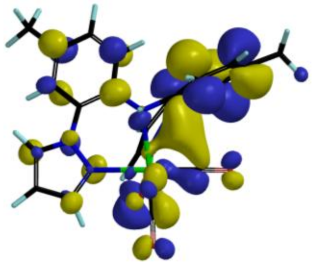	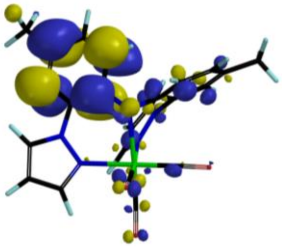	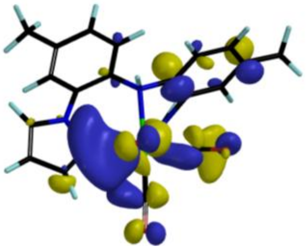
LUMO (+3)	**LUMO (+4)**	**LUMO (+5)**

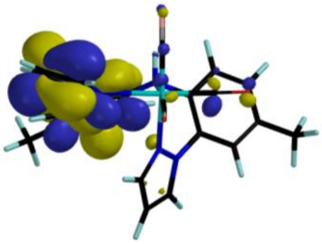	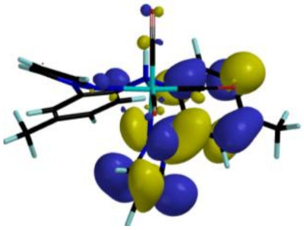	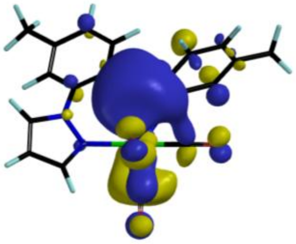
LUMO	**LUMO(+1)**	**LUMO(+2)**

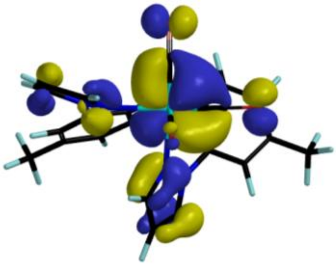	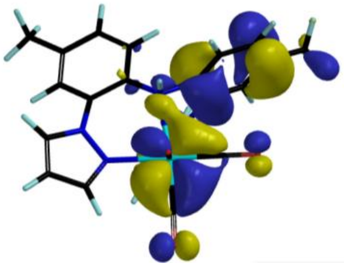	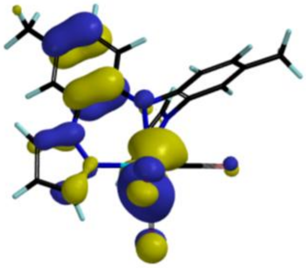
HOMO	**HOMO(-1)**	**HOMO(-2)**

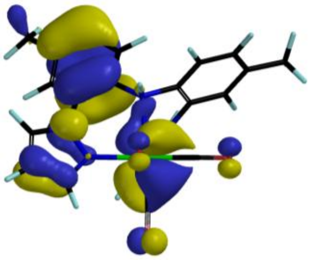	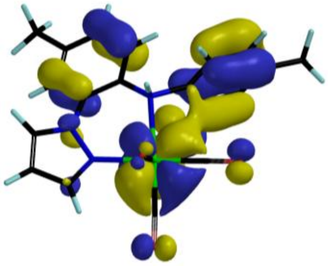	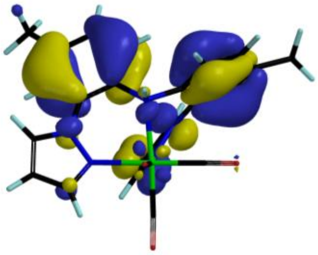
HOMO(-3)	**HOMO(-4)**	**HOMO(-5)**

Fig. S-19. Frontier Orbitals for Re(CO)$_3$(**L**) (**3**) from DFT calculations (B3LYP/LACVP*).

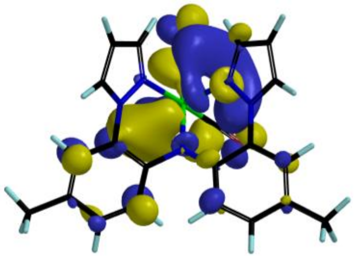	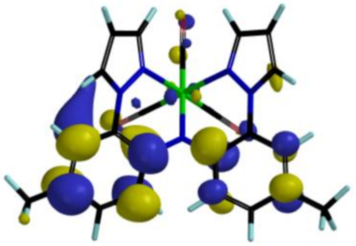	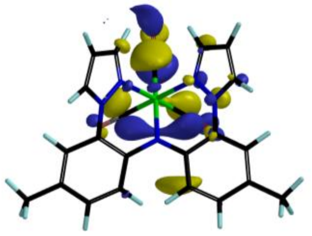
LUMO (+3)	**LUMO (+4)**	**LUMO (+5)**

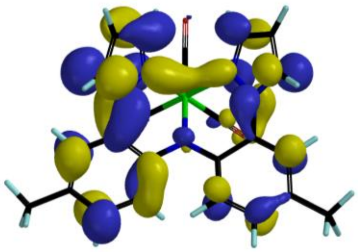	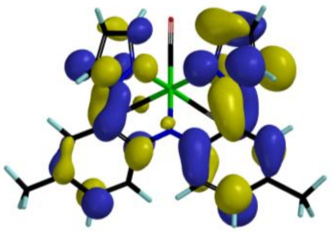	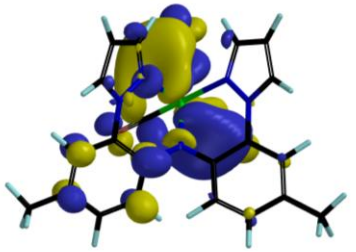
LUMO	**LUMO(+1)**	**LUMO(+2)**

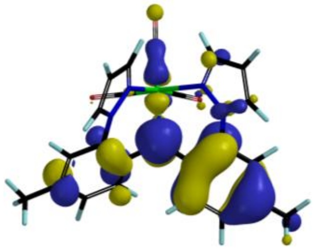	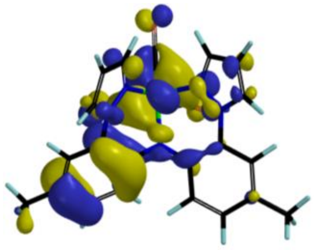	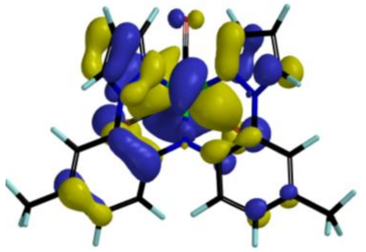
HOMO	**HOMO(-1)**	**HOMO(-2)**

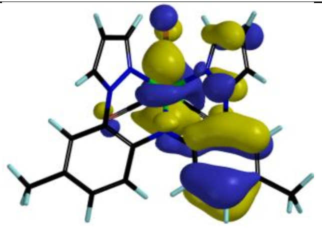	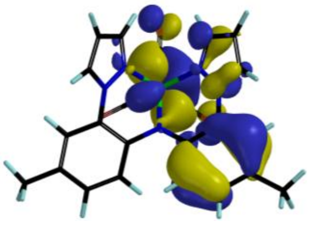	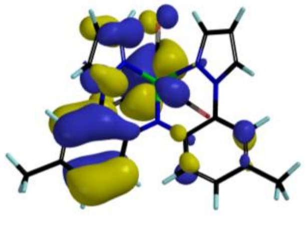
HOMO(-3)	**HOMO(-4)**	**HOMO(-5)**

Fig. S-20. Alpha Spin Frontier Orbitals for $[Re(CO)_3(\mathbf{L})]^+$ ($\mathbf{3}^+$) from DFT calculations (B3LYP/LACVP*).

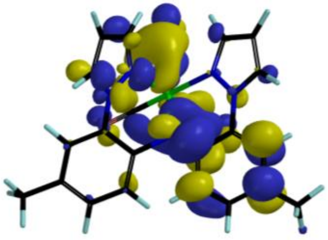	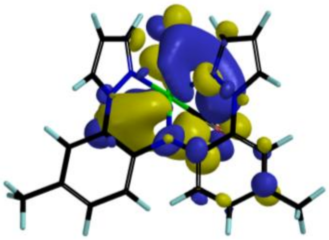	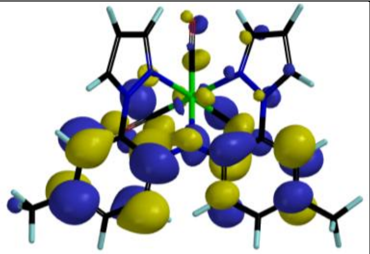
α-LUMO (+3)	**α-LUMO (+4)**	**α-LUMO (+5)**

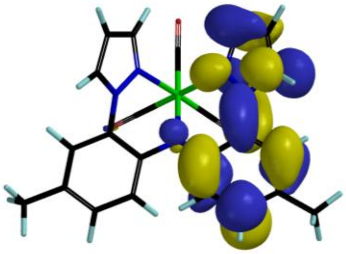	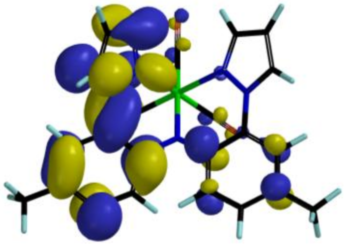	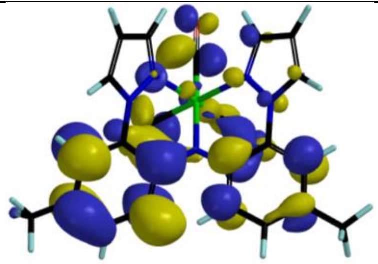
α-LUMO	**α-LUMO(+1)**	**α-LUMO(+2)**

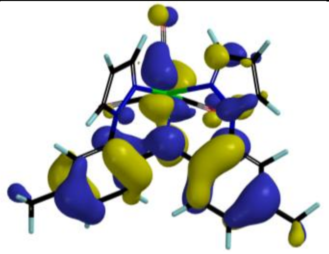	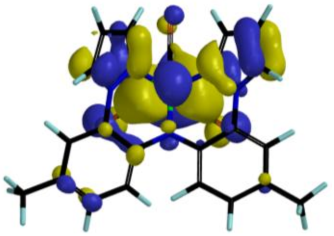	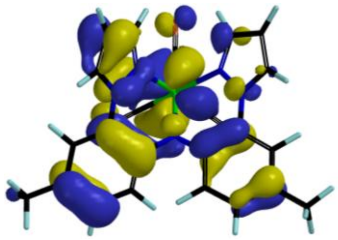
α-HOMO	**α-HOMO(-1)**	**α-HOMO(-2)**

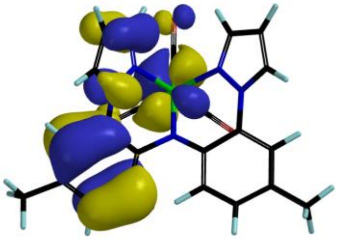	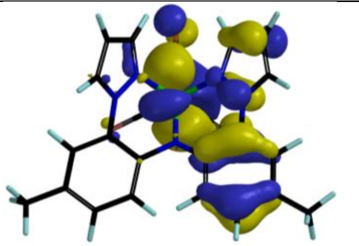	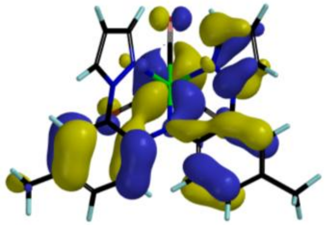
α-HOMO(-3)	**α-HOMO(-4)**	**α-HOMO(-5)**

Fig. S-21. Beta Spin Frontier Orbitals for [Re(CO)$_3$(**L**)]$^+$ (**3**$^+$) from DFT calculations (B3LYP/LACVP*).

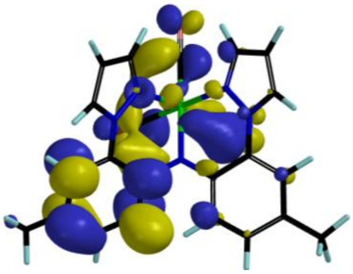	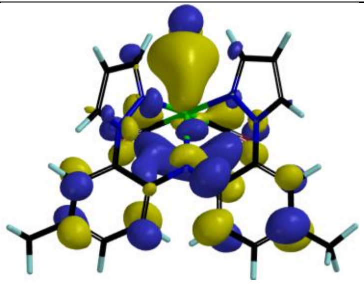	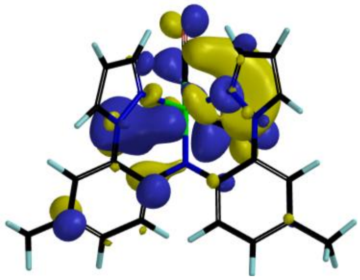
β-LUMO (+3)	**β-LUMO (+4)**	**β-LUMO (+5)**

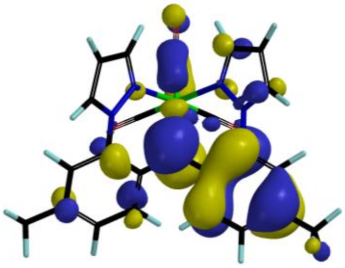	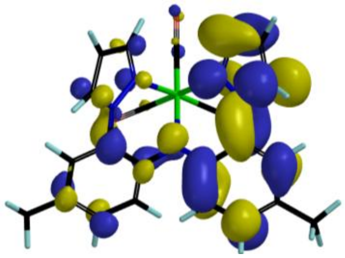	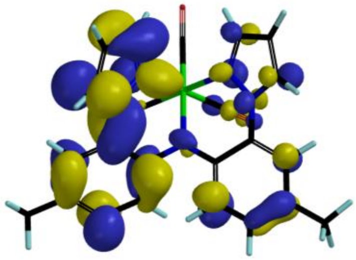
β-LUMO	**β-LUMO(+1)**	**β-LUMO(+2)**

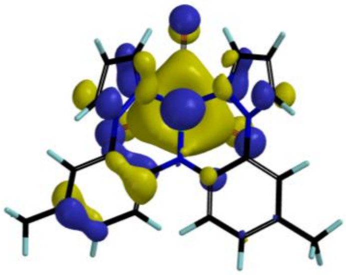	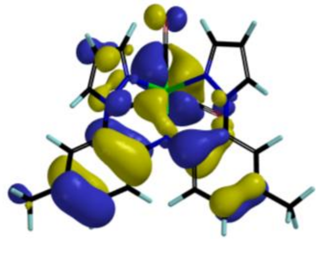	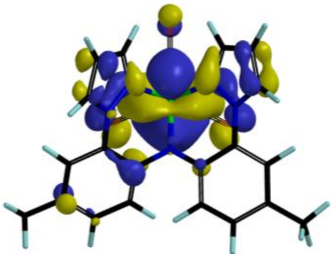
β-HOMO	**β-HOMO(-1)**	**β-HOMO(-2)**

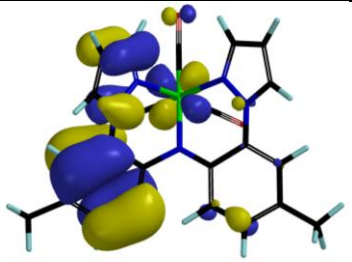	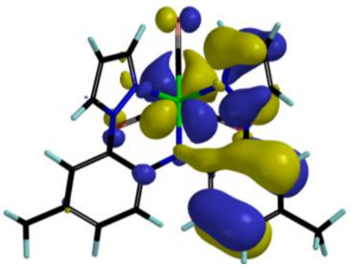	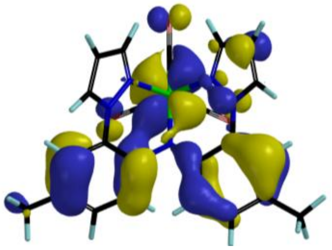
β-HOMO(-3)	**β-HOMO(-4)**	**β-HOMO(-5)**

Figure S-22. Simulated electronic absorption spectra of **1**, **2**$^+$, **3**, and **3**$^+$ fitted with Gaussian curves with full-width-at-half-maximum of 40 nm.

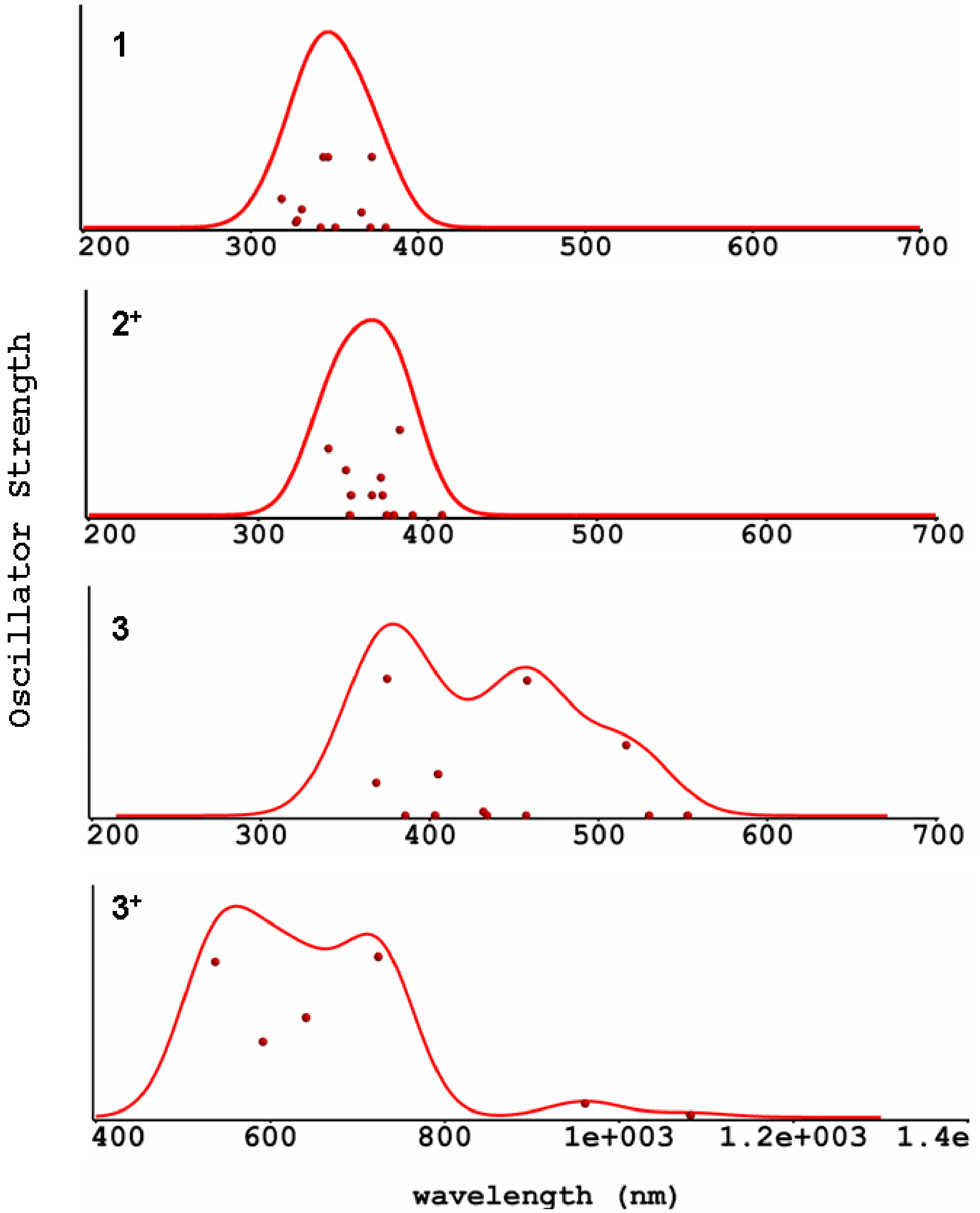

TDDFT/TDA Excitation Energies for 1

Excited state 1: excitation energy (eV) = 3.2566
Total energy for state 1: -1479.622018059532
Multiplicity: Triplet
Trans. Mom.: 0.0000 X 0.0000 Y 0.0000 Z
Strength : 0.0000
D(119) --> V(1) amplitude = 0.9556

Excited state 2: excitation energy (eV) = 3.3301
Total energy for state 2: -1479.619318640326
Multiplicity: Singlet
Trans. Mom.: 0.1484 X 0.2565 Y 0.1735 Z
Strength : 0.0096
D(119) --> V(1) amplitude = 0.9896

Excited state 3: excitation energy (eV) = 3.3372
Total energy for state 3: -1479.619058899995
Multiplicity: Triplet
Trans. Mom.: 0.0000 X 0.0000 Y 0.0000 Z
Strength : 0.0000
D(118) --> V(1) amplitude = 0.9466

Excited state 4: excitation energy (eV) = 3.3868
Total energy for state 4: -1479.617236331303
Multiplicity: Singlet
Trans. Mom.: -0.0257 X -0.0487 Y 0.1487 Z
Strength : 0.0021
D(118) --> V(1) amplitude = 0.9903

Excited state 5: excitation energy (eV) = 3.5366
Total energy for state 5: -1479.611728580531
Multiplicity: Triplet
Trans. Mom.: 0.0000 X 0.0000 Y 0.0000 Z
Strength : 0.0000
D(118) --> V(3) amplitude = -0.3066
D(118) --> V(4) amplitude = 0.2180
D(119) --> V(3) amplitude = 0.5487
D(119) --> V(4) amplitude = -0.4354
D(119) --> V(5) amplitude = -0.2929
D(119) --> V(6) amplitude = 0.2462

Excited state 6: excitation energy (eV) = 3.5811
Total energy for state 6: -1479.610093180668
Multiplicity: Triplet
Trans. Mom.: 0.0000 X 0.0021 Y 0.0000 Z
Strength : 0.0096
D(111) --> V(1) amplitude = -0.3308
D(114) --> V(1) amplitude = 0.3991
D(115) --> V(1) amplitude = 0.2687
D(116) --> V(1) amplitude = 0.4482
D(117) --> V(1) amplitude = 0.3440

Key: D(115) = HOMO, V(1) = LUMO
D(114) = HOMO(-1), V(2) = L(+1); etc.

Excited state 7: excitation energy (eV) = 3.6113
Total energy for state 7: -1479.608983753050
Multiplicity: Triplet
Trans. Mom.: 0.0096 X 0.0000 Y 0.0000 Z
Strength : 0.0096
D(118) --> V(3) amplitude = 0.6006
D(118) --> V(4) amplitude = -0.2998
D(118) --> V(5) amplitude = -0.4026
D(119) --> V(3) amplitude = 0.3342

Excited state 8: excitation energy (eV) = 3.6282
Total energy for state 8: -1479.608364006247
Multiplicity: Triplet
Trans. Mom.: 0.0000 X 0.0000 Y 0.0000 Z
Strength : 0.0000
D(114) --> V(2) amplitude = -0.3266
D(116) --> V(2) amplitude = 0.5812
D(117) --> V(2) amplitude = 0.2961
D(118) --> V(2) amplitude = 0.2227

Excited state 9: excitation energy (eV) = 3.7502
Total energy for state 9: -1479.603879107580
Multiplicity: Singlet
Trans. Mom.: -0.0779 X 0.0099 Y 0.1454 Z
Strength : 0.0025
D(119) --> V(2) amplitude = 0.7575
D(119) --> V(3) amplitude = -0.4618
D(119) --> V(4) amplitude = 0.2907

Excited state 10: excit. energy (eV) = 3.7823
Total energy for state 10: -1479.602701674650
Multiplicity: Singlet
Trans. Mom.: -0.1013 X 0.0130 Y -0.0128 Z
Strength : 0.0010
D(119) --> V(2) amplitude = 0.6030
D(119) --> V(3) amplitude = 0.6577
D(119) --> V(4) amplitude = -0.2617
D(119) --> V(5) amplitude = -0.2688

Excited state 11: excit. energy (eV) = 3.7916
Total energy for state 11: -1479.602357313963
Multiplicity: Singlet
Trans. Mom.: 0.0301 X 0.0180 Y -0.0796 Z
Strength : 0.0007
D(118) --> V(2) amplitude = 0.9253
D(118) --> V(4) amplitude = 0.2326

Excited state 12: excit. energy (eV) = 3.8940
Total energy for state 12: -1479.598596977632
Multiplicity: Singlet
Trans. Mom.: 0.0066 X -0.1926 Y 0.0605 Z
Strength : 0.0039
D(118) --> V(2) amplitude = 0.3097
D(118) --> V(3) amplitude = 0.7089
D(118) --> V(4) amplitude = -0.4187

TDDFT/TDA Excitation Energies for 2

Excited state 1: excitation energy (eV) = 3.0361
Total energy for state 1: -1466.353429882337
Multiplicity: Triplet
Trans. Mom.: 0.0000 X 0.0000 Y 0.0000 Z
Strength : 0.0000
D(115) --> V(1) amplitude = 0.9872

Excited state 2: excitation energy (eV) = 3.1701
Total energy for state 2: -1466.348505355361
Multiplicity: Triplet
Trans. Mom.: 0.0000 X 0.0000 Y 0.0000 Z
Strength : 0.0000
D(115) --> V(2) amplitude = 0.9768

Excited state 3: excitation energy (eV) = 3.2342
Total energy for state 3: -1466.346152520360
Multiplicity: Singlet
Trans. Mom.: 0.4473 X 0.3013 Y -0.1558 Z
Strength : 0.0250
D(115) --> V(1) amplitude = 0.9427
D(115) --> V(2) amplitude = 0.2445

Excited state 4: excitation energy (eV) = 3.2628
Total energy for state 4: -1466.345098410478
Multiplicity: Triplet
Trans. Mom.: 0.0000 X 0.0000 Y 0.0000 Z
Strength : 0.0000
D(114) --> V(1) amplitude = 0.6663
D(114) --> V(2) amplitude = 0.6822

Excited state 5: excitation energy (eV) = 3.2991
Total energy for state 5: -1466.343764711871
Multiplicity: Triplet
Trans. Mom.: 0.0250 X 0.0000 Y 0.0000 Z
Strength : 0.0000
D(114) --> V(1) amplitude = 0.7391
D(114) --> V(2) amplitude = -0.6300

Excited state 6: excitation energy (eV) = 3.3204
Total energy for state 6: -1466.342984703722
Multiplicity: Singlet
Trans. Mom.: -0.1553 X 0.1778 Y 0.1271 Z
Strength : 0.0058
D(113) --> V(1) amplitude = 0.2170
D(114) --> V(1) amplitude = -0.5361
D(115) --> V(2) amplitude = 0.7828

Key: D(115) = HOMO, V(1) = LUMO
D(114) = HOMO(-1), V(2) = L(+1); etc.

Excited state 7: excitation energy (eV) = 3.3299
Total energy for state 7: -1466.342634951297
Multiplicity: Singlet
Trans. Mom.: -0.3451 X 0.0899 Y 0.0839 Z
Strength : 0.0109
D(114) --> V(1) amplitude = 0.8302
D(115) --> V(2) amplitude = 0.4708

Excited state 8: excitation energy (eV) = 3.3778
Total energy for state 8: -1466.340873967388
Multiplicity: Triplet
Trans. Mom.: 0.0109 X 0.0058 Y 0.0000 Z
Strength : 0.0058
D(112) --> V(1) amplitude = 0.3153
D(113) --> V(1) amplitude = 0.8943

Excited state 9: excitation energy (eV) = 3.4955
Total energy for state 9: -1466.336549137390
Multiplicity: Singlet
Trans. Mom.: 0.2379 X 0.0836 Y -0.0727 Z
Strength : 0.0059
D(113) --> V(1) amplitude = 0.7007
D(114) --> V(2) amplitude = 0.6488

Excited state 10: excitation energy (eV) = 3.5018
Total energy for state 10: -1466.336315114806
Multiplicity: Triplet
Trans. Mom.: 0.0000 X 0.0000 Y 0.0000 Z
Strength : 0.0000
D(111) --> V(1) amplitude = 0.2770
D(112) --> V(1) amplitude = -0.5215
D(113) --> V(1) amplitude = 0.3122
D(113) --> V(2) amplitude = 0.6615

Excited state 11: excitation energy (eV) = 3.5240
Total energy for state 11: -1466.335502452611
Multiplicity: Singlet
Trans. Mom.: 0.3531 X -0.1666 Y 0.0113 Z
Strength : 0.0132
D(113) --> V(1) amplitude = 0.6017
D(113) --> V(2) amplitude = -0.4123
D(114) --> V(2) amplitude = -0.6004

Excited state 12: excitation energy (eV) = 3.6325
Total energy for state 12: -1466.331514831832
Multiplicity: Singlet
Trans. Mom.: 0.0767 X -0.4484 Y -0.1075 Z
Strength : 0.0194
D(113) --> V(2) amplitude = 0.8711
D(114) --> V(2) amplitude = -0.3270

TDDFT/TDA Excitation Energies for 3

Excited state 1: excitation energy (eV) = 2.2431
Total energy for state 1: -1465.352989987785
Multiplicity: Triplet
Trans. Mom.: 0.0000 X 0.0000 Y 0.0000 Z
Strength : 0.0000
D(115) --> V(1) amplitude = 0.9899

Excited state 2: excitation energy (eV) = 2.3402
Total energy for state 2: -1465.349423764482
Multiplicity: Triplet
Trans. Mom.: 0.0000 X 0.0000 Y 0.0000 Z
Strength : 0.0000
D(115) --> V(2) amplitude = 0.9872

Excited state 3: excitation energy (eV) = 2.4011
Total energy for state 3: -1465.347184678253
Multiplicity: Singlet
Trans. Mom.: -0.6578 X 0.3729 Y 0.0944 Z
Strength : 0.0342
D(115) --> V(1) amplitude = 0.9768

Excited state 4: excitation energy (eV) = 2.7098
Total energy for state 4: -1465.335842155477
Multiplicity: Singlet
Trans. Mom.: -0.6957 X -0.6940 Y -0.1474 Z
Strength : 0.0655
D(115) --> V(2) amplitude = 0.9415

Excited state 5: excitation energy (eV) = 2.7131
Total energy for state 5: -1465.335720453897
Multiplicity: Triplet
Trans. Mom.: 0.0000 X 0.0000 Y 0.0000 Z
Strength : 0.0000
D(115) --> V(3) amplitude = 0.9939

Excited state 6: excitation energy (eV) = 2.8580
Total energy for state 6: -1465.330395849302
Multiplicity: Triplet
Trans. Mom.: 0.0342 X 0.0655 Y 0.0000 Z
Strength : 0.0000
D(115) --> V(4) amplitude = 0.9818

Key: D(115) = HOMO, V(1) = LUMO
D(114) = HOMO(-1), V(2) = L(+1); etc.

Excited state 7: excitation energy (eV) = 2.8727
Total energy for state 7: -1465.329852633203
Multiplicity: Singlet
Trans. Mom.: 0.0862 X 0.1373 Y 0.0023 Z
Strength : 0.0018
D(115) --> V(3) amplitude = 0.9629

Excited state 8: excitation energy (eV) = 3.0622
Total energy for state 8: -1465.322890670511
Multiplicity: Singlet
Trans. Mom.: -0.1074 X 0.5055 Y -0.0351 Z
Strength : 0.0201
D(115) --> V(4) amplitude = 0.9233
D(115) --> V(5) amplitude = -0.2996

Excited state 9: excitation energy (eV) = 3.0756
Total energy for state 9: -1465.322398022733
Multiplicity: Triplet
Trans. Mom.: 0.0018 X 0.0201 Y 0.0000 Z
Strength : 0.0000
D(115) --> V(5) amplitude = 0.9686

Excited state 10: excitation energy (eV) = 3.2166
Total energy for state 10: -1465.317216329854
Multiplicity: Triplet
Trans. Mom.: 0.0000 X 0.0000 Y 0.0000 Z
Strength : 0.0000
D(114) --> V(1) amplitude = 0.9749

Excited state 11: excitation energy (eV) = 3.3077
Total energy for state 11: -1465.313867583838
Multiplicity: Singlet
Trans. Mom.: -0.8913 X 0.1401 Y -0.0688 Z
Strength : 0.0664
D(115) --> V(4) amplitude = 0.2753
D(115) --> V(5) amplitude = 0.8773

Excited state 12: excitation energy (eV) = 3.3664
Total energy for state 12: -1465.311711006372
Multiplicity: Singlet
Trans. Mom.: -0.2016 X 0.1215 Y 0.3706 Z
Strength : 0.0159
D(112) --> V(1) amplitude = 0.2309
D(114) --> V(1) amplitude = 0.9118

TDDFT/TDA Excitation Energies for 3$^+$

Key: D(114) = β-HOMO, S(1) = SOMO
D(113) = β-HOMO(-1) etc.

Excited state 1: excitation energy (eV) = 1.1461
Total energy for state 1: -1465.681866755314
<S**2> : 0.7820
Trans. Mom.: -0.0809 X 0.1636 Y 0.1911 Z
Strength : 0.0020
D(112) --> S(1) amplitude = -0.1781 beta
D(114) --> S(1) amplitude = 0.9801 beta

Excited state 2: excitation energy (eV) = 1.2901
Total energy for state 2: -1465.676572164976
<S**2> : 0.7809
Trans. Mom.: -0.4551 X 0.1278 Y 0.0430 Z
Strength : 0.0071
D(113) --> S(1) amplitude = 0.9862 beta

Excited state 3: excitation energy (eV) = 1.7128
Total energy for state 3: -1465.661039338508
<S**2> : 0.7819
Trans. Mom.: 0.3624 X 1.1215 Y 0.5938 Z
Strength : 0.0731
D(109) --> S(1) amplitude = 0.1662 beta
D(111) --> S(1) amplitude = -0.2267 beta
D(112) --> S(1) amplitude = 0.9259 beta
D(114) --> S(1) amplitude = 0.1717 beta

Excited state 4: excitation energy (eV) = 1.9338
Total energy for state 4: -1465.652918908972
<S**2> : 0.7870
Trans. Mom.: 0.9637 X 0.1472 Y 0.1230 Z
Strength : 0.0457
D(110) --> S(1) amplitude = -0.2854 beta
D(111) --> S(1) amplitude = 0.9185 beta
D(112) --> S(1) amplitude = 0.1875 beta

Excited state 5: excitation energy (eV) = 2.0953
Total energy for state 5: -1465.646981941635
<S**2> : 0.7907
Trans. Mom.: -0.0992 X 0.8173 Y -0.0029 Z
Strength : 0.0348
D(109) --> S(1) amplitude = -0.2139 beta
D(110) --> S(1) amplitude = 0.9042 beta
D(111) --> S(1) amplitude = 0.2718 beta
D(112) --> S(1) amplitude = 0.1638 beta

Excited state 6: excitation energy (eV) = 2.3094
Total energy for state 6: -1465.639114155231
<S**2> : 0.0020
Trans. Mom.: -0.9738 X -0.5118 Y -0.2052 Z
Strength : 0.0709
D(109) --> S(1) amplitude = 0.9367 beta
D(110) --> S(1) amplitude = 0.2490 beta

References.

[S1] S.P. Schmidt, W.C. Trogler, F. Basolo, *Inorg. Synth.* 1990, **28**, 160.

[S2] L. Fan, B.M. Foxman, O.V. Ozerov, *Organometallics* 2004, **23**, 326.

[S3] I. Noviandri, K.N. Brown, D.S. Fleming, P.T. Gulyas, P.A. Lay, A.F. Masters, L. Phillips, *J. Phys. Chem. B* 1999, **103**, 6713.

[S4] R. Rathore, C.L. Burns, M.I. Deselinescu, S.E. Denmark, T. Bui, *Org. Synth.* 2005, **82**, 1.

[S5] SMART APEX2 Version 2.0-2 Bruker Analytical X-ray Systems, Inc., Madison, Wisconsin, USA, 2005.

[S6] SAINT+ Version 7.23a and SADABS Version 2.05. TWINABS Bruker Analytical X-ray Systems, Inc., Madison, Wisconsin, USA, 2007.

[S7] Sheldrick, G. M. SHELXTL Version 6.1; Bruker Analytical X-ray Systems, Inc., Madison, Wisconsin, USA, 2000.

[S8] CCDC 759658, 759659, 759660, 759661, and 759662 contain the supplementary crystallographic data for **H(L)**, **1**, **2·PF$_6$**, **2·OTf**, and **3**. These data can be obtained free of charge from The Cambridge Crystallographic Data Centre via www.ccdc.cam.ac.uk/data_request/cif.

[S9] (a) B.J. Liddle, S. Waniarachchi, S.V. Lindeman, J.R. Gardinier, *J. Organomet.. Chem.* 2010, **695**, 53. (b) L. Wei, J. Babich, W.C. Eckelman, and J. Zubieta *Inorg. Chem.*, **2005**, *44*, 2198. (c) B. Machura, R. Kruszynski, M. Jaworska, P. Lodowski, R. Penczek, J. Kusz, *Polyhedron* 2008, **27**, 1767. (c) R.M. Silva, B.J. Liddle, S.V. Lindeman, M.D. Smith, J.R. Gardinier, *Inorg. Chem.* 2006, **45**, 6794.

[S10] SPARTAN, Wavefunction, Inc., Irvine, CA, 1997.

[S11] For instance see: (a) Ref S-9a. (b) T. Takatani, J. S. Sears, D. C. Sherill, *J. Phys. Chem. A* 2009, **113**, 9231. (c) V.M. Rayon, G. Frenking, *Chem. Eur. J.* 2002, **8**, 4693. (d) R.K. Szilagyi, G. Frenking, *Organometallics* 1997 **16**, 4807.

[S12] A. D. Becke, *J. Chem. Phys.* 1993, **98**, 5648.

[S13] C. Lee, W. Yang, R.G. Parr, *Phys. Rev. B* 1988, **37**, 785.

[S14] (a) P. J. Hay, W.R. Wadt, *J. Chem. Phys.* 1985, **82**, 270. (b) W.R. Wadt, P.J. Hay, *J. Chem. Phys.* 1985, **82**, 284.